ASSESSING COPPER AND ZINC ADSORPTION TO THERMALLY TREATED LIGNOCELLULOSIC BIOMASS

By

JOSEPH PAUL SMITH

A thesis submitted in partial fulfillment of
the requirements for the degree of

MASTER OF SCIENCE IN ENVIRONMENTAL ENGINEERING

WASHINGTON STATE UNIVERSITY
Department of Civil and Environmental Engineering

AUGUST 2015

To the Faculty of Washington State University:

The members of the Committee appointed to examine the thesis of JOSEPH PAUL SMITH find it satisfactory and recommend that it be accepted.

_____

David Yonge, Ph.D., Chair

_____

Richard J. Watts, Ph. D.

_____

Michael P. Wolcott, Ph. D.

ACKNOWLEDGMENTS

I would like to thank my advisor, David Yonge, and my committee members, Richard Watts and Michael Wolcott, for providing invaluable advice and guidance throughout my time at Washington State University. Among others who made this thesis possible, I would like to thank Vince MacIntyre, Manuel Garcia-Perez, Karl Englund, Scott Boroughs, Fang Chen, Jinxue Jiang, Ian Dallhiemer, Matt Smith, Wanda Terry, Janet Duncan, Suzanne Hamada, and Kelly Walsch. I am grateful to the Washington State Department of Transportation for funding the project. Lastly, thanks go to my parents, Paul and Beth Smith, and my sister, Stephanie Smith, for their moral support.

ASSESSING COPPER AND ZINC ADSORPTION TO THERMALLY TREATED LIGNOCELLULOSIC BIOMASS

Abstract

by Joseph Paul Smith, M.S.
Washington State University
August 2015

Chair: David Yonge

Anthropogenic activity in urban areas introduces high concentrations of contaminants, including dissolved metals, to stormwater runoff. Copper and zinc cations present in stormwater runoff should be treated to ensure a healthy environment and ecosystem for both human and aquatic life. Several stormwater best management practices have shown success for metal concentration reduction. Adsorption systems generally require a smaller footprint and are desired when space is restricted. This study evaluated the efficacy of two sorbents, torrefied wood and biochar, for their ability to adsorb metal contaminants. The sorbents' physical and chemical properties were defined by CO_2 adsorption surface area analysis, Fourier transform infrared (FTIR) spectrometry, and background metal concentrations. Sorbent surface area did not change during torrefaction (270 °C). However, pyrolysis (400 °C) yielded a surface area for biochar approximately 100 times greater than that of torrefied wood. FTIR showed the transformation of lignocellulosic material from the cellulosic to the ligneous fraction as sample treatment temperature increased, resulting in the formation of carboxylic acid functional groups in torrefied wood and biochar. Single- and multi-solute isotherm data and continuous flow column data was collected to quantify the sorbents' potential for metal removal. The Freundlich

equation was shown to yield the best fit of equilibrium data. Both single- and multi-solute isotherm data showed that for both torrefied wood and biochar, Cu yielded higher sorption capacities and outcompeted Zn. Through 10 simulated storm events performed in preliminary continuous flow columns, biochar had average removals of 91% Cu and 76% Zn, and torrefied wood had 67% Cu and 37% Zn average removals. The data indicated that torrefied wood and biochar show potential as metal sorbents for stormwater treatment and should be further evaluated in lab and pilot scale systems.

TABLE OF CONTENTS

LIST OF TABLES

LIST OF FIGURES

1 INTRODUCTION

Contaminants found in stormwater runoff typically include heavy metals, nutrients, petroleum hydrocarbons, biochemical oxygen demand, and suspended solids (Hallack, 2007). Zinc (Zn) and copper (Cu) are among the most common heavy metals present in stormwater runoff (Davis et al., 2001; Sansalone and Buchberger, 1997; Wisdom and Buchich, 2011, Yonge et al., 2002). Davis et al. (2001) examined typical sources of copper and zinc in stormwater runoff to determine the main contributors to metal loads. It was found that runoff from roofing and siding was the main contributor to copper loads. Automobile brake wear was the next highest copper contributor. The main contributor to zinc loads was runoff from roofing and siding, followed by automobile tire wear (Davis et al., 2001). Additionally, galvanized steel guardrails contribute to zinc loads. Studies have shown wide ranges of total (5-325 μg/L) and dissolved (5-280 μg/L) copper concentrations in urban and highway stormwater runoff. Even wider ranges of total and dissolved zinc, from 20-15,240 μg/L and 20-14,790 μg/L, respectively, have been reported (Barrett et al., 1998; Kayhanain et al., 2006; Marsalek et al., 1997; Sansalone and Buchberger, 1997; Wu et al., 1998).

If left untreated, stormwater runoff from these sources, particularly in densely populated urban areas may contain metal concentrations harmful to many species of aquatic organisms (Kori-Siakpere and Ubogu, 2008). A 2007 study performed by Sandahl et al. showed impairments to coho salmon resulting from an increase in aquatic Cu concentration (Sandahl et al., 2007). As the aquatic Cu concentration increased from 0.3 μg/L to 20 μg/L, responsiveness linked to olfactory sensitivity decreased. In 2007, Giardina et al. showed that elevated zinc

concentrations (5.72 mg/L compared to a control of 0.041 mg/L) have lethal effects on *Gambusia holbrooki* (Giardina et al., 2007). It was also noted that fish surviving elevated Zn concentrations exhibited decreased sperm motility. To protect aquatic species, The Washington Administrative Code has set acute and chronic dissolved copper concentration limits for discharge into marine water in the state of Washington at 4.8 µg/L and 3.1 µg/L, respectively (WAC 173-201A-240). Acute and chronic dissolved zinc concentration limits for discharge into marine are set at 90 µg/L and 81 µg/L respectively (WAC 173-201A-240). It is important to note that the discharge regulations are given for the soluble fraction because metal toxicity is attributed to dissolved forms.

Stormwater can be treated by both physical and chemical processes. Physical best management practices (BMPs) include street sweeping, filtration, and sedimentation, while the most common physiochemical BMP is adsorption (WSDOT, 2009). Sedimentation can be effective in removing metals associated with runoff particulates and dissolved metals that sorb to particulate matter during the settling process. Sedimentation ponds, however, require a relatively large footprint. In areas that offer little available space, adsorption by way of a packed bed column is a more practical strategy for dissolved metals removal.

Adsorption in a stormwater environment is defined as the transfer of a liquid phase contaminant (e.g. ion or molecule) to a solid phase. The contaminant attaches to the solid phase surface by physical and/or chemical processes. Soluble metal transfer, or partitioning, often occurs through ion exchange, in which cations with a smaller charge are replaced by cations with a larger charge. For example, Cu^{2+} may replace two Na^{+} molecules by bonding with two negative sites on a sediment surface. Electrostatic bonds can also be formed by divalent metal

cations bonding to two sites at which acidic functional groups containing R—OH have lost a hydrogen ion to become R—O^-. These principles can be applied to treat stormwater runoff containing metal ions of concern.

Numerous sorbents, including granular activated carbon (GAC), widely used in drinking water and wastewater treatment, have been shown to be effective at reducing metal ion concentrations in stormwater runoff (Liu et al., 2005). The effectiveness of GAC is due to its surface chemistry and high surface area, which can exceed 1000 m^2/g. However, production costs of GAC are significant. Recent stormwater treatment research has included experimentation on low-impact, inexpensive substrates that have sorption characteristics similar to GAC.

Several lower cost natural sorbents have been tested for treating metals present in stormwater runoff. These materials include tree bark, zeolites, sand, saw dust, and fern (Genc-Fuhrman et al., 2007; Ho et al., 2002; Yu et al., 2000). Yonge and Roelen (2003) found that a mixture of 90% sand, 5% clay, and 5% compost, by weight, was effective in treating highway stormwater runoff. While the mixture was effective, it presented relatively low infiltration rates and could have been outperformed by other sorbents, including GAC. In an effort to discover an even more effective low-impact development treatment option, materials with properties similar to GAC were considered for this project. Biochar, a carbonaceous byproduct of pyrolysis biofuel production with high specific surface area, has properties resembling GAC and would be more cost effective due to the nature of its production.

Biofuels have been garnering attention as an alternative energy source in an effort to reduce fossil fuel dependence (Czernik and Bridgewater, 2004). Fast pyrolysis of solid biomass feedstock is one of the production methods that have been studied in recent years (Lehmann, 2007). The pyrolysis process involves heating biomass (e.g. wood, grass, corn husks) in various reactor systems at temperatures ranging from 400 to 500 °C at zero or low oxygen partial pressure for relatively short time periods, typically on the order of minutes. These systems are often purged with nitrogen gas to control oxygen partial pressure within the reaction chamber. During the heating process, volatile components are released from the biomass feedstock. The volatiles are subsequently condensed as biofuel. After pyrolysis, what remains of the biomass feedstock is a carbon rich, porous substance known as biochar (Dumrose et al., 2011; Lehmann 2007). While biochar was initially repurposed as charcoal briquettes, the scope of possible applications for biochar has been expanding in recent years (Dumrose et al., 2011; Lehmann 2007). For example, biochar has shown an affinity for metal sorption (Karami et al., 2011; Tong et al., 2011). Tong et al. used Fourier transform infrared spectroscopy (FTIR) and zeta potential studies to show that copper was adsorbed through surface complexations, agreeing with the knowledge that metals are adsorbed through ion exchange and other surface chemical processes (Watts, 1998).

A milder form of pyrolysis, known as torrefaction, occurs at temperatures between 225 and 300 °C (Phanphanich and Mani, 2011). Torrefaction has emerged as a novel way to enhance the value of biomass as a fuel source (Phanphanich and Mani, 2011). Before torrefaction, biomass has a low energy density (8-14 MJ/kg) and high moisture content (25-60 %) due to its hygroscopic nature. As the biomass is heated, volatiles are released and the solid product

(torrefied wood) contains an increased energy density (up to 23 MJ/kg). The increased energy density improves the economics of shipping and handling biomass as a fuel source. Biomass in its original state has a high oxygen to carbon (O/C) ratio (Prins et al., 2006) compared to coal and other fuels that have low O/C ratios and are more effienct. As biomass is torrefied and volatiles are released, the O/C ratio is decreased. Though the main function of torrefied wood has been energy densification and improved fuel efficiency of biomass sources, there is evidence that suggests altered surface structures on torrefied woods can yield an effective sorbent (Chen et al., 2014; Haoxi and Ragauskas, 2011; Park et al., 2013).

The Washington Department of Transportation (WSDOT) is considering new adsorbents in an effort to discover sustainable and low impact development options for dissolved metals removal from runoff specifically related to state ferry terminal parking lots and queuing lanes. Optimizing adsorbent performance will minimize space requirements, which is a necessity in ferry terminal settings. The following study serves as a characterization and assessment of biochar and torrefied wood as a means of metal adsorption for stormwater treatment. Phase I of the project, presented herein, is focused on quantifying the adsorption of Cu and Zn on biochar and torrefied wood.

2 EXPERIMENTAL METHODS

Physical and chemical properties of biochar and torrefied wood were characterized to determine their affinity for metal adsorption. Physical characteristics were described by scanning electron microscopy (SEM), CO_2 liquid phase adsorption isotherms, and constant head hydraulic conductivity tests. Fourier transform infrared spectroscopy (FTIR) spectroscopy and

wet microwave digestion were performed to assess the sorbents' chemical properties. Copper and Zn adsorption isotherms provided information on the materials' abilities to adsorb metals in a well-mixed batch reactor. Preliminary flow-through column testing was used to indicate the sorbents' performance in a practical stormwater treatment application.

2.1 MATERIALS

Biochar and torrefied wood were tested for their ability to adsorb metals. The biochar was commercially obtained from Biochar Products, Halfway, OR. Communication with the supplier indicated that the biochar was produced from beetle-killed lodgepole pine using a 1 ton per day reactor manufactured by Abri Tech, Inc. (Namur, QC, Canada). The reactor used an auger with 2 mm steel heat carriers, no carrier gas, and was operated at 400 °C with a total system residence time of five to seven minutes (Englund and Dumroese, Personal Communication, 2015). In preparation for experimental testing, the bulk biochar sample was dried at 103 °C for 24 hours before being sieved to a size fraction between an 8 mesh and 6 mesh (2.36 and 3.35 mm) US Series sieve.

Two mm douglas fir Crumbles®, obtained from Forest Concepts, LLC, Auburn, WA, were torrefied at Washington State University in a Lindberg/Blue M Tube Furnace (Asheville, NC) at 270 °C with a residence time of 30 minutes in an air atmosphere. Air was supplied from a compressed air tank at a flow of 4.5 ± 0.5 liters per minute. The torrefied wood was sieved to the size retained on a 10 mesh (2.00 mm) US Series sieve. Untreated 2 mm douglas fir will be referred to as raw wood. Photographs of biochar, raw wood, and torrefied wood are shown in Figure 1.

Figure 1: Representative images of the three materials tested in this study.

2.2 SEM AND SURFACE AREA ANALYSIS

SEM was performed on the materials to allow for visual analysis of surface structure. Imaging was afforded by an FEI Quanta 200 scanning electron microscope. To improve conductivity, the torrefied wood and raw wood were gold sputtered prior to scanning. The biochar conductivity allowed it to be imaged without sputtering. CO_2 surface area adsorption tests were performed using a TriStar II plus automatic physisorption analyzer (Micromeritics Instrument Corporation, Norcross, GA). In preparation for testing, materials were dried for 8 hours at 200 °C. CO_2 isotherms were then collected at 273 K with partial pressure between 0.0001 and 0.03 atm.

2.3 FTIR AND METAL ANALYSIS OF SORBENTS

FTIR spectroscopy, used to define sorbent surface functional groups, was conducted at a resolution of 4 cm^{-1} and 32 scans on a Thermo Nicolet Nexus 670 spectrometer. Samples were prepared for analysis by grinding and collecting material that passed a 60 M (<0.250 mm) US Series sieve. A 3 mg sample was then mixed with 300 mg KBr and formed into a transparent pellet for transmission analysis.

Background metals contained in each sorbent were determined by wet microwave digestion using a CEM SP-D system. Prior to microwave digestion, 2 mL of 30% reagent grade H_2O_2 was added to a 35 mL quartz digestion vessel, followed by 200 mg sample and 3 mL 69-71% reagent grade HNO_3. The system then operated for one hour at 400 PSI, 220 °C, and a power of 300 W. Following the digestion procedure, the solutions were analyzed for metals using Inductively Coupled Plasma – Mass Spectrometry (ICP-MS) (see Chapter 2.4.2).

Sorbent metal analysis was also performed using United States Environmental Protection Agency (USEPA) method 200.7 that determines total recoverable analytes from solid samples. As such, 1 g of dried sample was added to a 250 mL Phillips beaker. Four mL of 1:1 HNO_3:DI water and 10 mL of 1:4 HCl:DI water were added to the beaker before being gently refluxed at 95 °C for 30 minutes. The samples were diluted to a known volume with 18 MΩ DI water and filtered using a 0.45 μm mixed cellulose ester filter paper. Metal concentrations were determined using ICP-MS (see Chapter 2.4.2).

2.4 ADSORPTION EQUILIBRIUM AND KINETICS

2.4.1 Batch Equilibrium Experiments

The equilibrium adsorption capacities of biochar and torrefied wood were determined for this study using the standard adsorption isotherm technique where a known concentration and volume of sorbate is contacted with a known mass of sorbent at constant temperature. Adsorption isotherm data was generated at room temperature (20±1°C) using a series of 250 mL amber glass packer bottles with Teflon-lined caps. All bottles contained a known mass of sorbent, solution volume, and initial concentration of sorbate. The bottles were placed on a tumbling table operating at approximately 15 inversions per minute for 24 hours. Figure 2 is a photograph of the tumbling table used in adsorption equilibrium and kinetics testing.

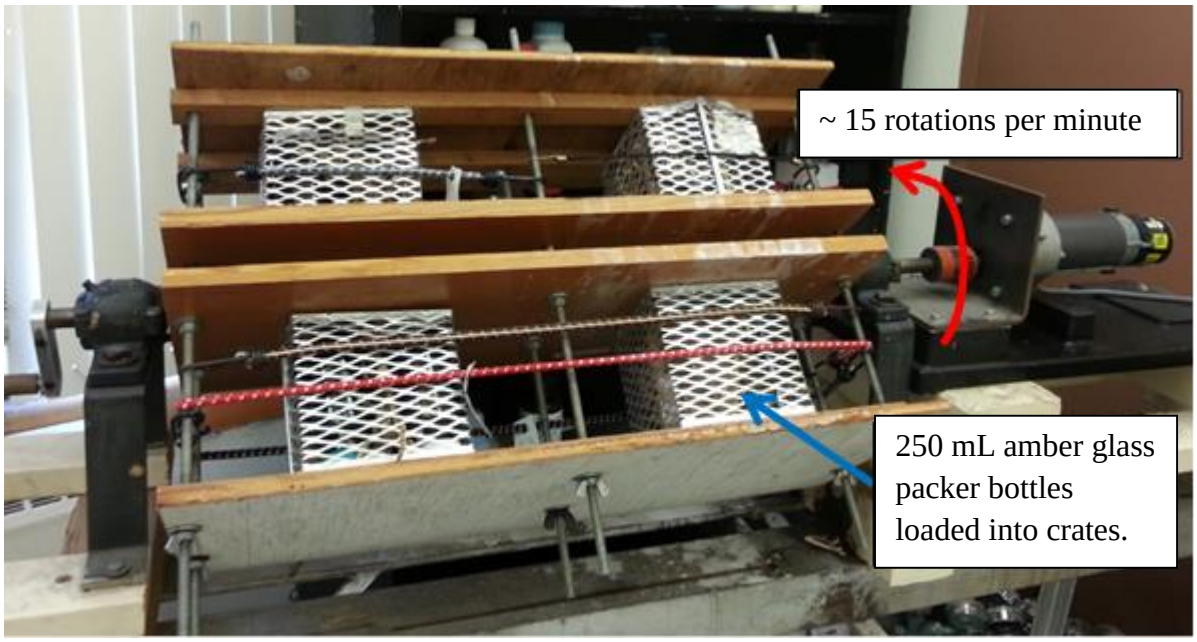

Figure 2: Tumbling table used to mix adsorption isotherm and kinetics samples. The motor was set to allow for approximately 15 full rotations per minute.

Copper and Zn stock solutions (1000 mg/L) were prepared using reagent grade $CuCl_2 \cdot 2H_2O$ and $ZnCl_2$ (Fischer Scientific) dissolved in 18 MΩ deionized (DI) water. The stock solutions were diluted with DI water containing 0.01 M $NaNO_3$, yielding a typical ionic strength found in stormwater (Liu et al., 2005), to a total solute volume of 200 mL at predetermined initial liquid phase concentrations. A known mass of sorbent and a predetermined volume of 1 M NaOH or 1 M HNO_3 was added to each bottle so that the pH following equilibration would be between 6.0 and 6.5 (Hach HQ411d pH meter). Initial liquid-phase metal concentrations and sorbent masses for single- and multi-solute systems are presented in Table 1. Experiments conducted to determine required acid or base volumes and equilibration times are presented in Appendix A.

Table 1: Initial liquid phase metal concentrations and sorbent masses used for single-solute and multi-solute systems. Note: due to a shortage of sorbent, only two Cu single-solute tests were performed on 1g and 3g biochar.

Metal System	**Target Initial Liquid Phase Metal Concentration (mg/L)**	**Sorbent Masses (g)**	**Sorbent Masses Tested in Triplicate (g)**
Single Solute, Cu	Cu – 7	1, 2, 3, 4, 5	1, 3, 5
Single Solute, Zn	Zn – 10	1, 2, 3, 4, 5, 7, 9	1, 3, 5
Multi-solute, Cu & Zn	Cu – 2.5 Zn – 4.5	1, 2, 3, 4, 5	1, 3, 5

For both single- and multi-solute systems, triplicate control bottles were tested using previously stated procedures but without sorbent. The results indicated negligible sorption to bottle walls and the cap liner. Additionally, all glassware was cleaned by soaking overnight in 20% (v/v) HNO_3 and rinsed with 18 MΩ DI water, per USEPA method 200.7.

2.4.2 Apparatus

Liquid phase metal concentraions were measured by ICP-MS using an Agilent 7700 ICP-MS. Prior to analysis, all samples were filtered through a 0.45 µm mixed cellulose esters filter (GE Healthcare) and acidified to pH less than or equal to 2, per USEPA method 200.7. Metal sorption to the filters was tested by placing one filter paper in a bottle containing a Cu and Zn solution of 110 and 360 µg/L, respectively. The bottle was mixed on the rotating table for 24 hours. Copper and Zn concentrations indicated insignificant sorption.

2.4.3 Adsorption Equilibrium Data Analysis

Following equilibration and quantification of the liquid phase sorbate concentration, the solid phase equilibrium concentration is calculated using equation 1,

$$q_e = \frac{(C_o - C_e)V}{m} \quad (1)$$

where q_e is the equilibrium solid phase concentration (mg sorbate/g sorbent), C_e is the equilibrium liquid phase concentration (mg/L), C_o is the initial liquid phase concentration (mg/L), V is the sorbate volume (L), and m is the mass of sorbent (g).

The Langmuir and Freundlich equations are commonly used to predict adsorption equilibrium. The predictive equations can then be used for treatment design. The Langmuir equation (equation 2) is based on fundamental principles of thermodynamics and assumes monolayer sorption.

$$q_e = \frac{QbC_e}{1 + bC_e} \tag{2}$$

where Q is the maximum solid phase capacity (mg sorbate/g sorbent) and b is the Langmuir adsorption constant of adsorbate (L/mg). Parameters Q and b can be determined by doing a linear transformation on experimental data. When plotted as C_e/q_e vs C_e, the slope equals 1/Q and the y-intercept equals 1/(Qb). Additionally, Q and b can be determined by changing their values using non-linear regression to minimize the residual sum of squares (RSS) between observed and predicted data. RSS can be quantified using equation 3,

$$RSS = \Sigma (y_{data} - y_{predicted})^2 \tag{3}$$

where the best overall model fit coincides with the smallest RSS.

The Freundlich equation (equation 4) is empirical and allows for multilayer adsorption.

$$q_e = K_F C_e^{1/n} \tag{4}$$

where K_F is the Freundlich adsorption capacity parameter $(mg/g)(L/mg)^{1/n}$, often expressed as (mg/g), and 1/n is the Freundlich adsorption intensity parameter (unitless), determined by logarithmically plotting experimental data (Watts, 1998). When plotted as log q_e vs log C_e, the

slope equals 1/n and the y-intercept equals log K_F. Values of K_F and 1/n can also be determined by non-linear regression as discussed above.

Equation constants and determination of the best fit equation (Langmuir or Freundlich) was accomplished using the RSS technique through application of the Solver function in Excel.

2.4.4 Adsorption Kinetics

Adsorption kinetics for Cu and Zn on biochar and torrefied wood was tested to determine if the 24 hour equilibrium period was sufficient. The general setup used for kinetics testing was the same as for the equilibrium experiments. A series of 15 replicate bottles containing initial Zn and Cu concentrations of 4.5 and 2.5 mg/L respectively, and 1.5 grams sorbent were mixed using the rotating table. Triplicate bottles were sacrificed at 6, 12, 24, 48, and 72 hour intervals. Triplicate bottles without sorbent, sacrificed at 6, 24, and 72 hours, showed negligible sorption to the bottle walls and cap liner.

2.5 HYDRAULIC CONDUCTIVITY AND PRELIMINARY COLUMN TESTING

2.5.1 Hydraulic Conductivity

Hydraulic conductivities of the biochar and torrefied wood were tested using a constant head method that was originally developed for soils with relatively high permeability (ASTM Standard D2423, 2000). Figure 3 shows a simplified schematic of the hydraulic conductivity testing setup.

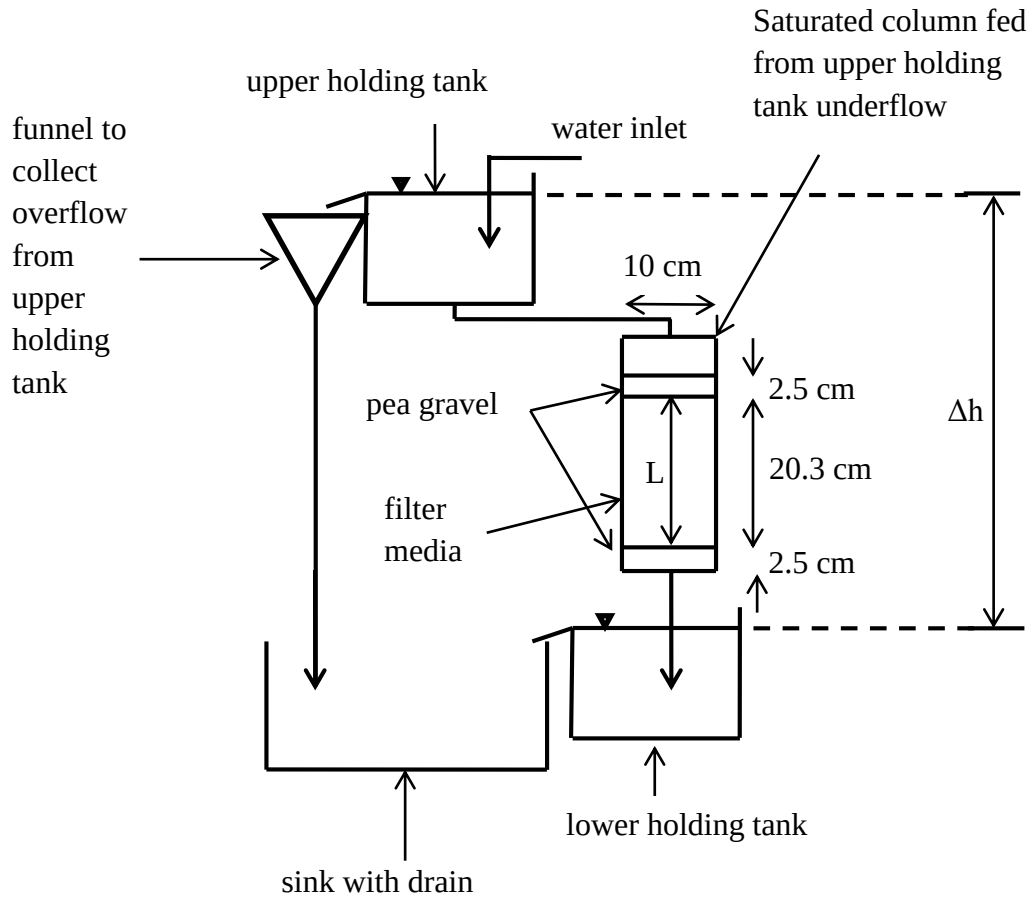

Figure 3: Simplified schematic of the hydraulic conductivity setup.

Material to be tested was placed into 10 cm diameter columns that were subsequently capped and sealed to create an air-tight system. An air release valve was included to release air pressure trapped when the column was capped. With the column effluent tube plugged and the air valve open, the column was filled with water until all air had been displaced, at which time the air release valve was closed. Next, a five minute equilibration period was completed for each material by flushing the column to allow for complete saturation and to wash fine particles from the column. Each experiment was conducted three times at five different Δh values (132, 140,

147, 155, and 163 cm). Flow through the material was measured at the lower holding tank overflow with a bucket and stopwatch at each Δh.

Using known values of flow, column dimensions, and Δh, the permeability coefficient, k (cm/sec), can be calculated using equation 5,

$$k = \frac{qL}{A\Delta h} \tag{5}$$

where q is the flow through the column (cm^3/second), L is the depth of material in the column (cm), A is the cross-sectional area of the column (cm^2), and Δh is the constant hydraulic head (cm). Cross-sectional area was calculated using equation 6,

$$A = \frac{\pi D^2}{4} \tag{6}$$

where D is the column Diameter (cm). The permeability coefficient was adjusted from the temperature recording during experimentation to the value at 20°C using equation 7,

$$k_{20} = k_T \frac{\mu_T}{\mu_{20}} \tag{7}$$

where μ_T/μ_{20} is the ratio of the kinematic viscosity of water at experimental temperature to the kinematic viscosity of water at 20 °C. Water viscosity values were interpolated from a set of data providing data for viscosity at 5 °C intervals (Kestin et al., 1978).

2.5.2 Continuous Flow Metal Adsorption

Preliminary column metal adsorption testing was completed using an unbuffered influent solution that consisted of 2 MΩ DI water with initial target concentrations of 300 µg/L Zn and 50

μg/L Cu, which are within recorded ranges of dissolved metal concentrations in runoff (Kayhanain et al., 2006; Marsalek et al., 1997; Sansalone and Buchberger, 1997). The influent solution was prepared in 208 L Nalgene® drums using predetermined volumes of 1000 mg/L Cu and 1000 mg/L Zn stock solutions. pH was adjusted to within a range of 5.8 and 6.3 using 1 M NaOH. The influent solution was then allowed to equilibrate for at least 24 hours prior to use.

Biochar and torrefied wood columns were packed in triplicate to a constant height of 20.3 cm using a vibrating table (1 minute vibration period) and topped with 5.1 cm pea gravel. To hold the material in place, two layers of fiberglass screen were attached to the bottom of each column using hose clamps. Each column received ten simulated storm events, each lasting 20 minutes, at a flow of 0.76 L/min. There was a rest period of 24 hours between events, with the exception of a 72 hour rest period between events 5 and 6. As shown in Figure 4, a dual-head peristaltic pump allowed for one biochar column and one torrefied wood column to receive simultaneous influent flows, which were pumped through PVC piping and vinyl tubing to plastic shower head applicators at 0.76 L/min. The application rate of 96 L/min-m^2 lies within the range of application rates common for rapid sand filtration in drinking water treatment plants (Crittenden et al., 2012). Composite effluent samples were taken over the 20 minute loading period and preserved according to USEPA method 200.7. Metal sorption to tubing and columns was evaluated by performing experiments without sorbent. Analysis of the effluent samples indicated negligible sorption to the column and tubing. Additional analysis indicated that negligible metals concentrations leached from the piping and tubing system during events.

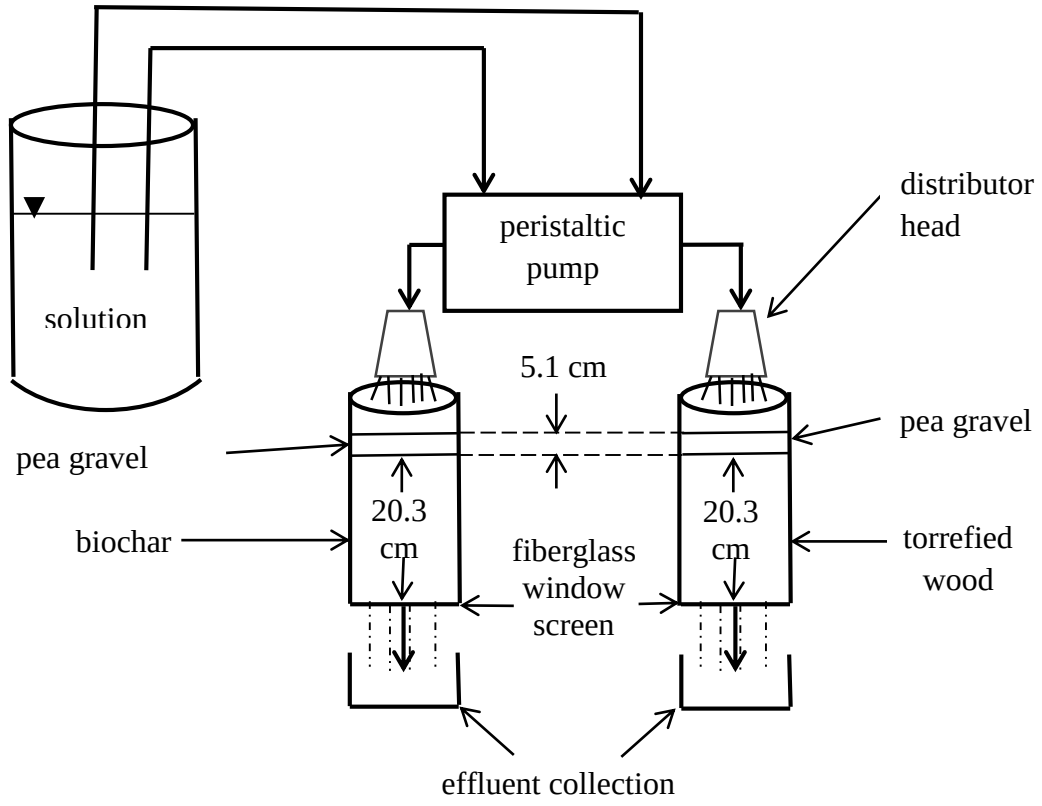

Figure 4: Simplified schematic of the flow-through column setup.

3 RESULTS AND DISCUSSION

3.1 SEM AND SURFACE AREA

SEM imaging results for raw wood, torrefied wood, and biochar are depicted in Figure 5. The images, presented at 500-x and 5000-x magnification, show the materials' cross-sectional surfaces. Observed differences between raw wood, torrefied wood, and biochar can be seen, but care must be taken in drawing conclusions as there are inherent anatomical differences between douglas fir (raw and torrefied wood) and lodgepole pine (biochar). Images taken at 500-x magnification show that both torrefied wood and biochar retain the majority of gross anatomical

properties during thermal treatment. Images taken at 5000-x magnification show that torrefied wood retains wood fiber ultrastructures while biochar does not. These structures degrade at elevated treatment temperatures as the structure of biomass is driven to elemental carbon.

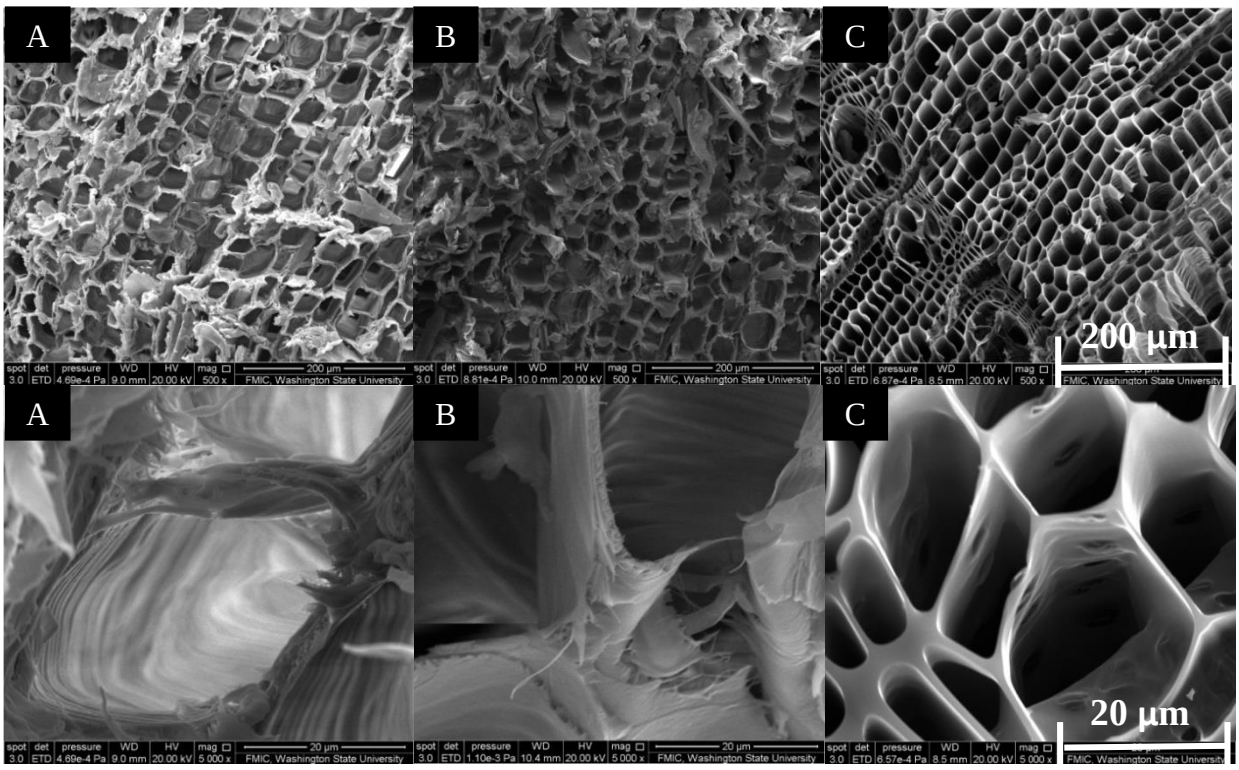

Figure 5: SEM micrographs at 500-x magnification (top row) and 5000-x magnification (bottom row) for A) raw wood, B) torrefied wood, and C) biochar.

CO_2 adsorption isotherms were generated to quantify the specific surface area and micropore (pores less than 2 nm in diameter) volume of biochar, which were found to be 395 m^2/g and 0.05 cm^3/g, respectively. Extensive experimentation with torrefied wood under a variety of conditions showed that surface area does not dramatically change during the torrefaction process, remaining at about 3-4 m^2/g. The low surface area is due to a lack of formation of micropores (Chen et al., 2011; Dallmeyer and Smith, Personal Communication,

2015). For this reason, CO_2 adsorption isotherms were not completed for the torrefied or raw wood used herein. Specific surface area values for raw and torrefied woods from other studies are presented in Table 2.

Common temperature ranges (200-300 °C) used for torrefaction do not alter the inner pore structure and micropore volume of the feedstock, which does occur at the higher pyrolysis temperature (400 °C) used to produce biochar. A 2012 literature review of the physical properties of biochar demonstrated the trends that specific surface area increases as reaction temperature increases, and that micropore volume increases as specific surface area increases (Downy et al, 2012). Downy et al. also concluded that an increased micropore volume was the greatest factor contriubuting to increased total surface area. Consequently, biochar has a greater specific surface area (approximately 100 times greater) than torrefied wood and raw wood because of the opening of its inner pore structure combined with the formation of micropores.

Activated carbon (AC) is essentially biochar that has been exposed most commonly to steam at temperatures ranging from 600 – 1200 °C. The result is the formation of fissures in the carbonaceous material that yield a complex inner pore structure, formation of more micropores, and a significantly elevated specific surface area. For treatment applications, AC is granulated and becomes GAC. The micropore volume of biochar used herein was found to be 0.05 cm^3/g and the surface area was consequesntly smaller, at 395 m^2/g. The surface area and micropore volume is consistent with literature data complied by Downy et al. (2012). In contrast, a GAC sample evaluated by Pradhan and Sandle had a micropore volume of 0.60 cm^3/g and a surface area of 1416 m^2/g (Table 2).

Table 2: Measured specific surface area of biochar and literature values of specific surface area of raw wood, torrefied wood, and GAC.

Material	Specific Surface Area (m^2/g)	Micropore Volume (cm^3/g)	Source
Biochar	395	0.05	This study
GAC	785 - 1416	0.60	Genc-Fuhrman et al., 2007; Pradhan and Sandle (1999)
Raw Wood (Willow)	3.9 ± 0.8	—	Jones et al., 2012
Torrefied Wood (Willow)	3.4 ± 0.4	—	Jones et al., 2012
Biochar (Willow)	270	—	Jones et al., 2012

3.2 SORBENT SURFACE CHEMICAL AND METALS ANALYSIS

3.2.1 Surface Chemistry

Thermal treatments degrade hemicellulose (200-260 °C), cellulose (240-350 °C), and lignin (280-500 °C) in wood cell walls (Colom, 2003). At treatment temperatures above 240°C, the carbohydrate fraction of the wood decreases, and the aromatic fraction present in lignin increases. Additionally, ether (R-O-R') bonds that link guaiacyl rings in lignin are thermally cleaved and newly formed C-C direct bonds are thought to increase the guaiacyl ring density (Park et al., 2013). Surface area available for potential adsorption sites increases with increased aromatic density in wood cell walls (Downy et al., 2012). Additionally, metal adsorption is enhanced on sorbents containing carboxyl functional groups that provide sites for ion exchange. The formation of carboxyl groups is a result of the degradation of carbohydrates in cellulose, and can be improved through oxygenation during or after thermal treatment (Toles et al., 1999). Figure 6 shows the structures of carboxylic acid and guaiacyl rings.

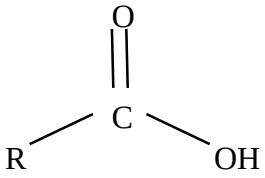

Carboxylic Acid

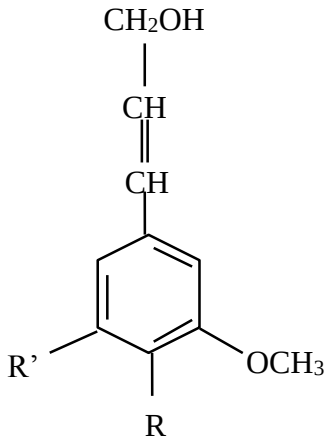

Guaiacyl Ring

Figure 6: Structures of carboxylic acid and guaiacyl rings. Guaiacyl rings are the backbone of lignin.

Results from FTIR analysis of raw wood, torrefied wood, and biochar, presented in Figure 7, indicate the stretching of a C=C bond in guaiacyl rings (1510 and 1600 cm^{-1}). While little can be said regarding absorbance at 1510 cm^{-1}, the peak at 1600 cm^{-1} was less intense for raw wood than for torrefied wood and biochar. Differences in peak intensity indicate an increased aromatic density in torrefied wood and biochar (Colom et al., 2003; Park et al., 2013). The fraction of cellulose, indicated by the presence of aliphatic C-O-C (1050 cm^{-1}) is typically inversely correlated to aromatic density. In this case, the peak was more intense in raw wood than in torrefied wood, and was no longer present in biochar. The results agree with the findings of others that indicate as treatment temperature increases, cellulose degrades and the aromatic content of the wood cell wall increases (Park et al., 2013). Additionally, the peak describing the presence of carbonyl (R-COR') groups (1740 cm^{-1}) was only present in raw wood suggesting a removal of ester groups (R-COOR') from the hemicellulose fraction as treatment temperature

increases above 200 °C (Park et al., 2013). Carboxylic acids (1700 cm^{-1}) are only present in the torrefied wood and biochar samples. This agrees with findings that as treatment temperature increases, the carbohydrate fraction of lignocellulosic biomass further degrades (Park et al., 2013).

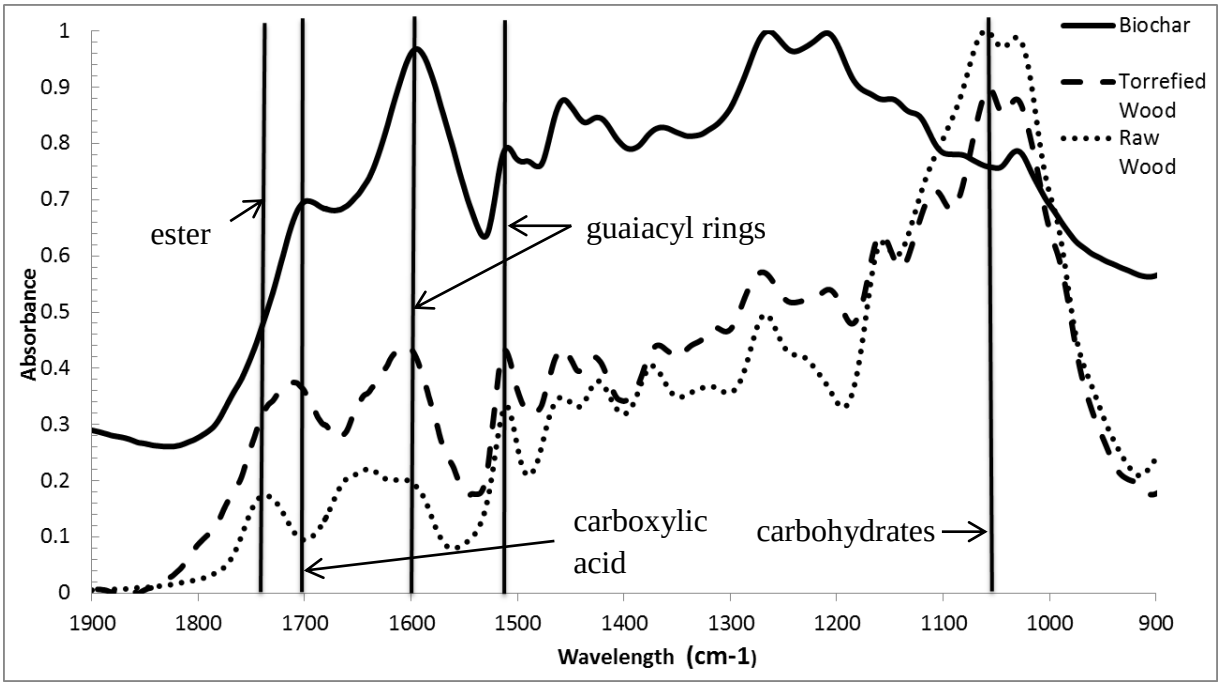

Figure 7: FTIR results from wavelengths 900 to 1900 cm^{-1} for biochar, torrefied wood, and raw wood. The absorbance at 1050 cm^{-1} relates to the carbohydrate fraction present in cellulose. Guaiacyl ring density is related to absorbance at 1510 and 1600 cm^{-1}. Carboxylic acid formation is described by absorbance at 1700 cm^{-1} and the presence of carbonyl groups (as ester) is described by absorbance at 1740 cm^{-1}.

3.2.2 Sorbent Metal Analysis

Genc-Fuhrman et al. noted that it is important to quantify baseline sorbent metal concentrations prior to adsorption experiments because the potential for certain metals to leach from a sorbent can limit its usefulness (Genc-Fuhrman et al., 2007). These baseline metals

concentrations were quantified for raw wood, torrefied wood, and biochar using microwave wet digestion. In addition, total recoverable metals analysis was performed on unused torrefied wood and biochar (EPA Method 200.7). The results, presented in Table 3, focus on three toxic metals (Cu, Pb, Zn) present in raw and torrefied wood and in biochar. Compared to torrefied wood, biochar contained less Cu and considerably more Zn. Mass loss associated with volatilization during torrefaction and pyrolysis would likely have concentrated metals in torrefied wood and biochar. Additional factors including difference in wood species and material handling and preparation could have contributed to the metal concentration differences seen in torrefied wood and biochar (Su, 2012). The concentrations of Cu and Zn in torrefied wood and biochar from microwave digestion and EPA Method 200.7 were consistent with the exception of the Zn concentration in biochar. The difference could be due to slight variations in the bulk biochar sample. A study by Hiraju et al. (1996) revealed that various metal concentrations exist within the same species and even the same tree.

Table 3: Metal analysis results for raw wood, torrefied wood, and biochar. BDL indicates a value measured below the detection limit of an analyte. "-" indicates no recorded data.

Analyte	Concentration (μg/L)					
	Microwave Digestion			EPA Method 200.7		
	Raw wood	Torrefied wood	Biochar	Raw wood	Torrefied wood	Biochar
Cu	BDL	26	10	-	23	8
Pb	BDL	5	BDL	-	-	-
Zn	5	2	38	-	5	118

3.3 ADSORPTION EQUILIBRIUM ISOTHERMS

Adsorption equilibrium data is often fit to Langmuir and Freundlich predictive equations for treatment system design purposes. These equations have been used to describe Cu and Zn adsorption by Genc-Fuhrman et al., (2007), Mohan and Singh (2002), and Yu et al., (2000). Data generated in this study for Cu and Zn adsorption to biochar and torrefied wood was fit to Langmuir and Freundlich equations.

3.3.1 Langmuir and Freundlich Equation Best Fit Analysis

Langmuir and Freundlich constants were determined using single solute Cu and Zn adsorption isotherm data by minimizing the RSS using non-linear regression. The RSS values for biochar and torrefied wood indicate that the Freundlich equation yielded the best fit of the single-solute adsorption data (Table 4).

Table 4: RSS values for single solute Cu and Zn isotherm data fit to Langmuir and Freundlich equations.

Adsorbent	**Biochar**		**Torrefied wood**	
	Cu	*Zn*	*Cu*	*Zn*
Langmuir	7.09×10^{-3}	0.01	2.22×10^{-3}	0.02
Freundlich	1.88×10^{-3}	8.24×10^{-3}	2.22×10^{-3}	3.52×10^{-3}

The data in figures 8 and 9 show Cu and Zn isotherm data with associated Langmuir and Freundlich equation predictions for biochar and torrefied wood. The experimental data is presented with 95% confidence intervals (CI). The large CI for one Cu data point on Figure 8 is due to a small sample size (n=2), necessary because of a shortage of sorbent.

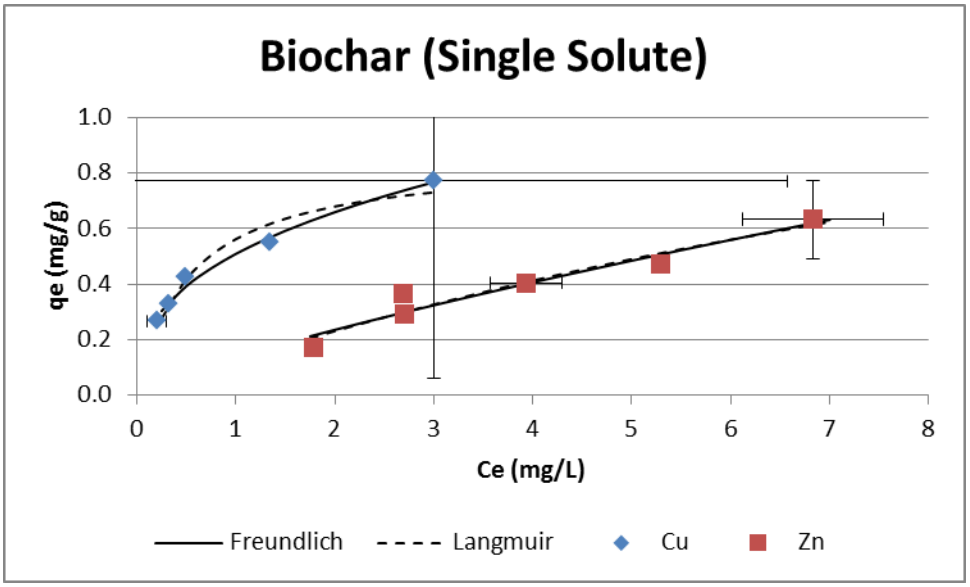

Figure 8: Biochar single solute Cu and Zn isotherm data and Langmuir and Freundlich equation preditions. Initial Cu and Zn concentrations were 7 mg/L and 10 mg/L, respectively. Data points are presented with 95% CI. A small sample size (n=2) contributed to the large CI seen for one Cu data point.

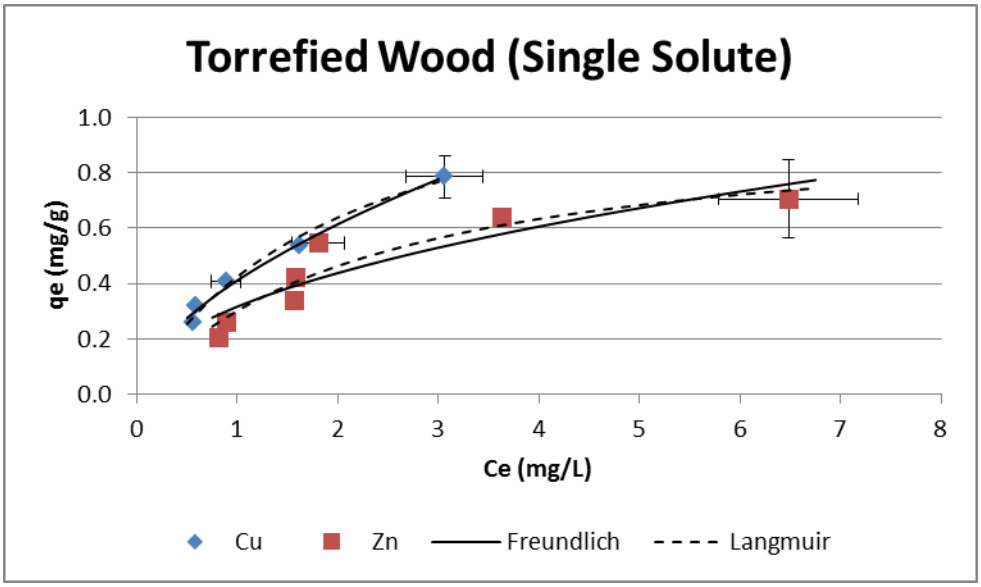

Figure 9: Torrefied wood single solute Cu and Zn isotherm data and Langmuir and Freundlich equation predictions. Initial Cu and Zn concentrations were 7 mg/L and 10 mg/L, respectively. Data points are presented with 95% CI.

Best fit values for K_F and 1/n are summarized in Table 5. Although K_F and 1/n are empirical curve fitting constants, K_F can be related to adsorption capacity. The data for this study shows that biochar had K_F values for Cu and Zn of 0.509 and 0.136, respectively. Torrefied wood had K_F values for Cu and Zn of 0.412 and 0.317, respectively. It can therefore be said that for both biochar and torrefied wood, in a single-solute system, Cu exhibits a greater adsorption capacity compared to Zn. The data in Figure 10 indicate that Cu has a greater affinity for biochar than torrefied wood, especially at lower C_e values. As expected, the value of K_F for Cu sorption on biochar is greater than that of torrefied wood. Conversely, the data in Figure 11 and associated K_F values indicate that Zn has a greater affinity for torrefied wood compared to biochar. It should be noted that while these results are presented based on a mass per mass and mass per volume basis, values are sometimes presented as moles per mass and moles per volume for a better comparison of sorption capacities. This was not done here because the mass per mass comparisons remain valid for Cu and Zn because their molecular weights only differ by 2.8%.

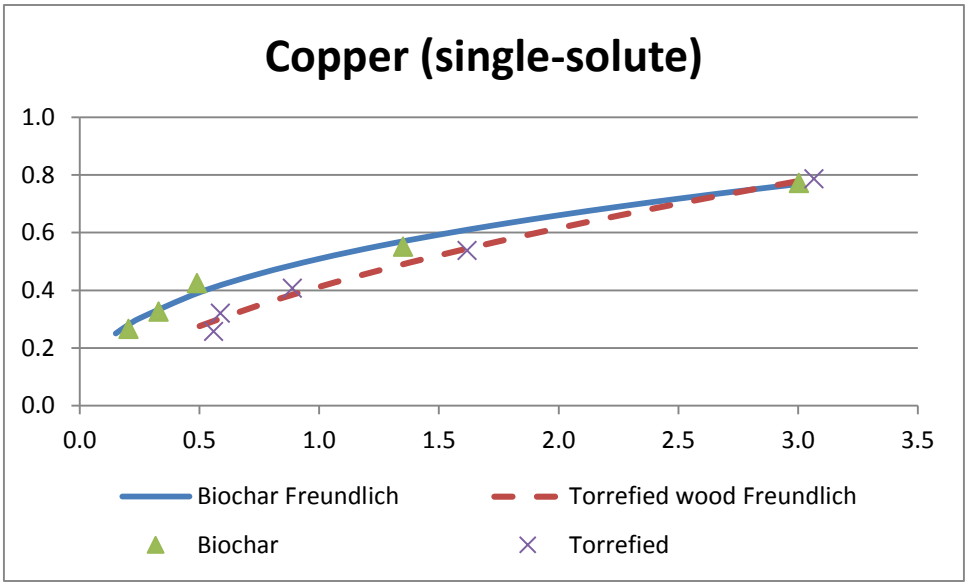

Figure 10: Comparison of biochar and torrefied wood Cu adsorption data.

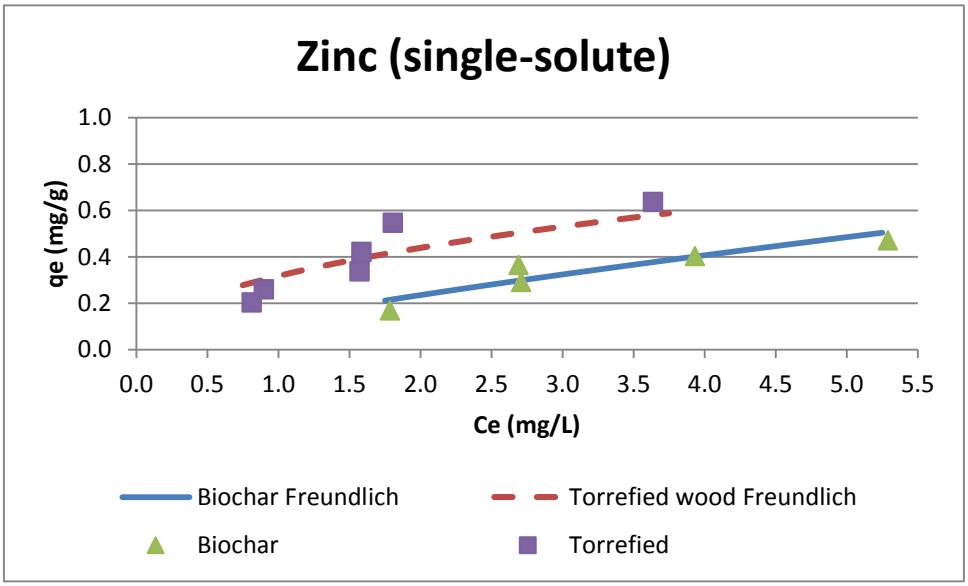

Figure 11: Comparison of biochar and torrefied wood Zn adsorption data.

The data in Table 5 allows comparisons to be made between the Freundlich constants found for biochar and torrefied wood and literature Freundlich constants for various other sorbents. It is interesting to note that K_F values for biochar and torrefied wood are similar to those reported for Cu adsorption on GAC (Genc-Fuhrman et al., 2007). Zinc adsorption on GAC, however, was significantly greater (Genc-Fuhrman et al., 2007; Mohan and Singh, 2002). Adsorbents have a greater affinity for certain metals over others. The preferential adsorption, known as the lyotrophic series, is related to particle charge and size. However, there is evidence that sorbents can have varying lyotropic series, particularly regarding divalent cation adsorption (Watts, 1998). Another example of varying lyotropic series between sorbents can be seen when comparing biochar and torrefied wood to natural zeolites tested by Genc-Fuhrman et al. (2007). K_F values for Cu sorption to biochar and torrefied wood were 4 and 3 times greater than the K_F value for Cu sorption to natural eolite. However, the K_F value for Zn sorption to natural zeolite was 2.5 and 1.15 times greater than the K_F values for biochar and torrefied wood, respectively.

Table 5: Freundlich constants for biochar and torrefied wood, presented with literature values for various sorbents.

Material	**Cu**		**Zn**		**Source**
	K_F (mg/g)	**1/n**	**K_F (mg/g)**	**1/n**	
Biochar	0.509	0.374	0.136	0.789	This Study
Torrefied Wood	0.412	0.579	0.317	0.468	This Study
Results from Similar Studies Below					
GAC	-	-	5.62	0.2516	Mohan and Singh (2002)
GAC	0.37	1.25	0.91	1.010	Genc-Fuhrman et al. (2007)
Natural Zeolite	0.13	1.471	0.36	0.870	Genc-Fuhrman et al. (2007)
Sand	0.1	0.637	0.03	0.730	Genc-Fuhrman et al. (2007)
Saw Dust (Maple)	0.956	0.601	-	-	Yu et al. (2000)
Sand/Clay/Compost Mix	0.282	0.622	0.057	0.031	Yonge and Roelen (2003)

3.3.2 Multi-Solute Adsorption Isotherms

Multi-solute isotherm data was plotted in conjunction with Freundlich equation predictions developed from single-solute Cu and single-solute Zn isotherm data (Figures 12 and 13). The multi-solute data generated from sorption to biochar and torrefied wood clearly shows that for both sorbents, Cu outperforms Zn in a competitive environment. Solid phase capacity for Cu on biochar in a multi-solute system remained essentially the same as in the single-solute system. Conversely, Zn sorption to biochar was negatively affected by the presence of Cu, evidenced by the data falling below the single-solute Freundlich equation prediction line. This indicates that Cu significantly outcompetes Zn in the multi-solute system studied herein. Similar results are shown for the torrefied wood (Figure 13). Preferential copper adsorption could help biochar and torrefied wood meet stringent limits set by the WAC for dissolved Cu discharge to marine waters.

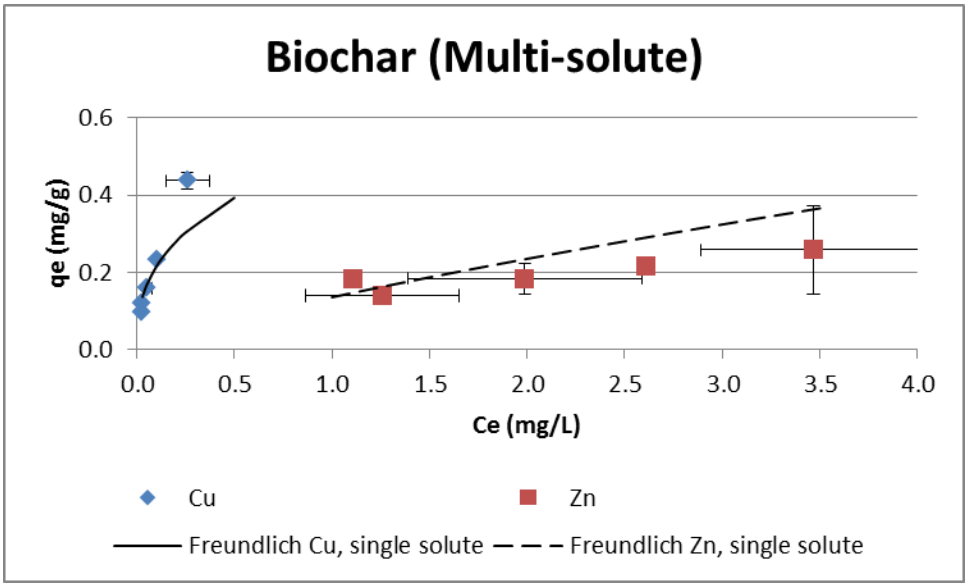

Figure 12: Biochar multi-solute isotherm data fit with single-solute Freundlich equations. Initial Cu and Zn concentrations were 2.5 and 4.5 mg/L, respectively. Data is presented with 95% CI.

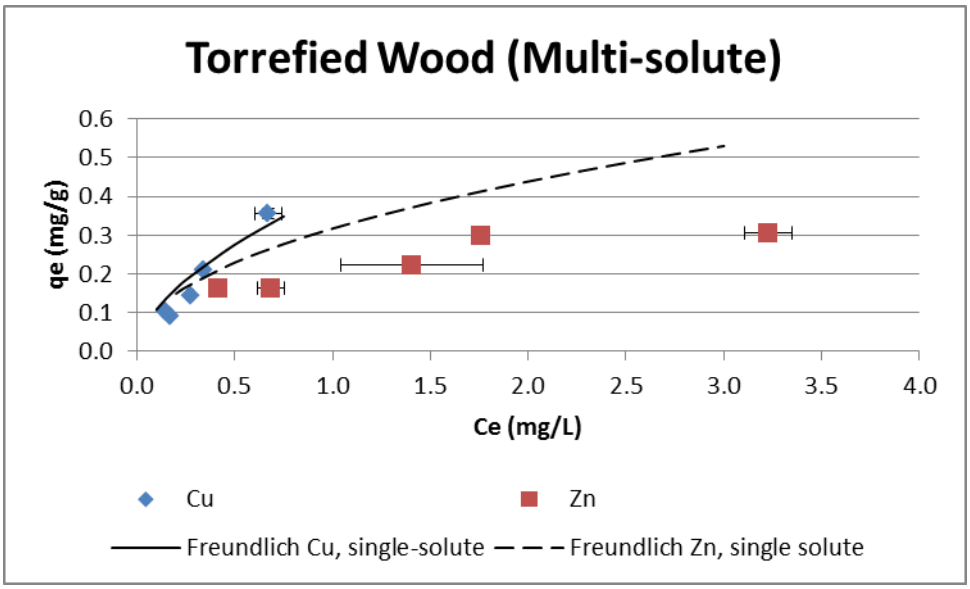

Figure 13: Torrefied wood multi-solute isotherm data fit with single-solute Freundlich equations. Initial Cu and Zn concentrations were 2.5 and 4.5 mg/L, respectively. Data is presented with 95% CI.

3.3.3 Adsorption Kinetics

The adsorption kinetics of Cu and Zn adsorption to biochar and torrefied wood were tested to assess if the 24 hour equilibrium period was sufficient to obtain useful data. Results are presented in Figures 14 and 15. At the 24 hour sample, 88% of Cu and 71% of Zn were adsorbed by biochar when compared to a 72 hour sample. After 24 hours, 91% of Cu and 90% of Zn were adsorbed by torrefied wood when compared to 72 hours. It was determined that while equilibrium had not been fully achieved, a 24 hour mixing period was sufficient to make comparisons between the performance of biochar and torrefied wood and to gain useful multisolute sorption data.

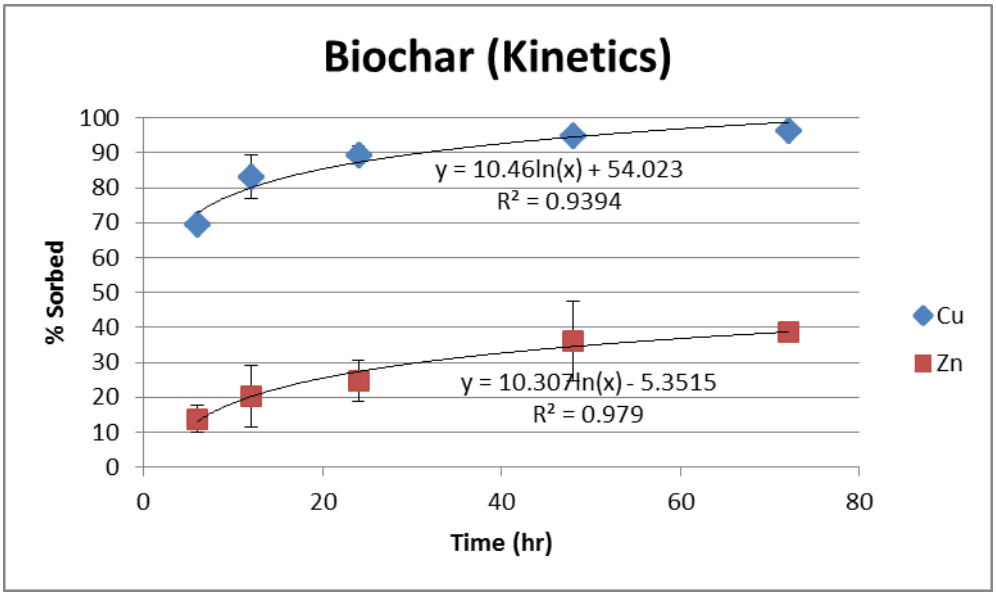

Figure 14: Biochar adsorption kinetics over 72 hours. Initial Cu and Zn concentrations were 2.5 and 4.5 mg/L, respectively. Data is presented with 95% CI.

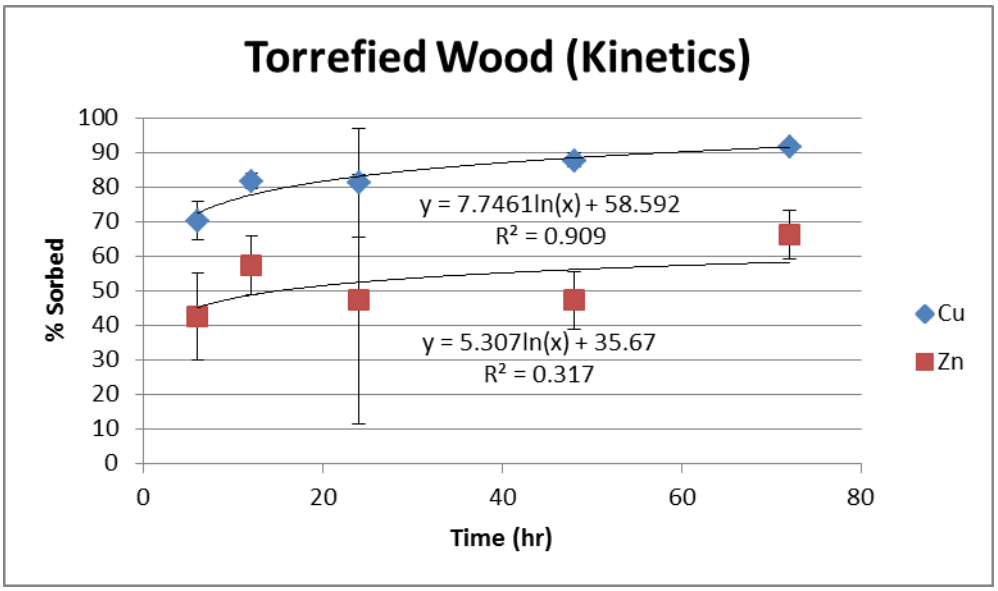

Figure 15: Torrefied wood adsorption kinetics over 72 hours. Initial Cu and Zn concentrations were 2.5 and 4.5 mg/L, respectively. Data is presented with 95% CI.

3.4 HYDRAULIC CONDUCTIVITY AND PRELIMINARY COLUMN TESTING

3.4.1 Hydraulic Conductivity

Constant head hydraulic conductivity testing was performed to understand maximum infiltration rates for biochar, torrefied wood, and raw wood. Biochar, torrefied wood, and raw wood had respective permeabilities of 0.669 ± 0.012 cm/sec, 0.359 ± 0.006 cm/sec, and 0.368 ± 0.006 cm/sec. Biochar exhibited the largest permeability due to the larger particle size of the material (2.36 – 3.35 mm) relative to raw and torrefied wood (2 mm). The torrefaction process had no effect on the permeability of the wood. The infiltration for torrefied wood fits within the range of rapid sand filters used in drinking water treatment, which are typically operated at 0.140 to 0.417 cm/sec (Crittenden et al., 2012). However, based on flow alone, biochar would be able to handle higher magnitude storms.

3.4.2 Continuous Flow Multicomponent Adsorption

Preliminary column tests were completed to gain an understanding of Cu and Zn sorption in continuous flow environments. At the start of a column experiment, the time measured between initiation of flow to the column and flow exiting the column was approximately 20 seconds, indicating a short contact time. Figures 16 and 17 present influent and effluent concentrations of Cu and Zn. The Cu and Zn effluent concentrations are an average of three replicate experiments for biochar and torrefied wood. The overall average percent Cu and Zn removals for biochar over 10 events were 91% and 76%, respectively. Average percent removals for torrefied wood over 10 events were 67% Cu and 37% Zn.

While biochar outperformed torrefied wood over the 10 simulated events, the performance of the torrefied wood columns improved with passing events. During events three through ten, the effluent torrefied wood concentrations decreased until they more closely resembled the effluent biochar concentrations. This was unexpected and will be discussed later. It should be noted that the error bars surrounding a number of average effluent Cu and Zn concentrations from torrefied wood columns are larger than the error bars surrounding average effluent Cu and Zn concentrations from biochar columns. A possible explanation is that the distribution shower heads that fed influent to the torrefied wood columns, which were a different brand than those that fed influent to biochar, underperformed on occasional events and resulted in channeling and less solute contact with the media.

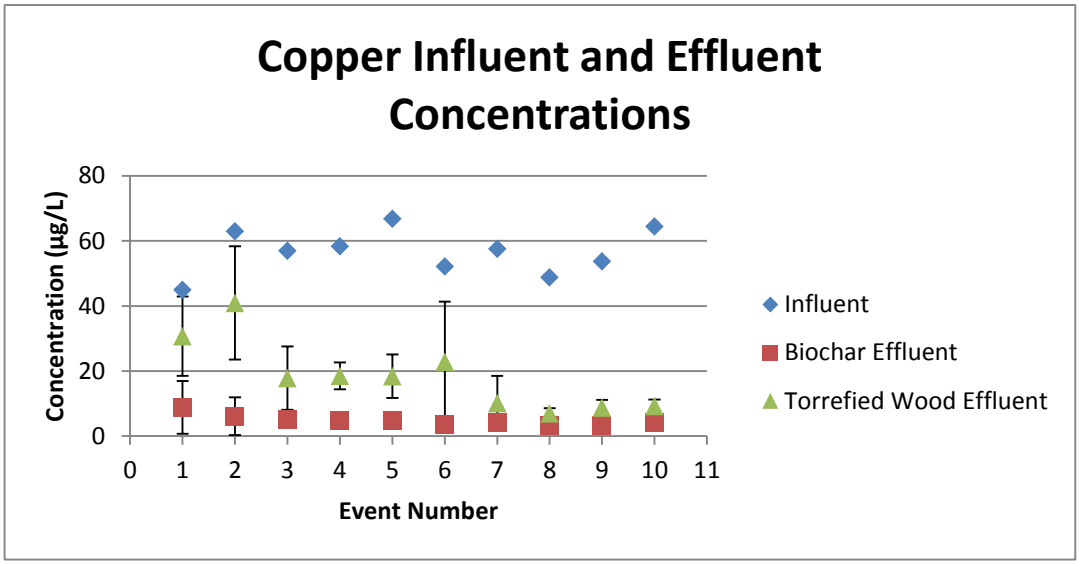

Figure 16: Average influent and effluent concentrations for 10 simulated storm events. Data is presented with 95% CI.

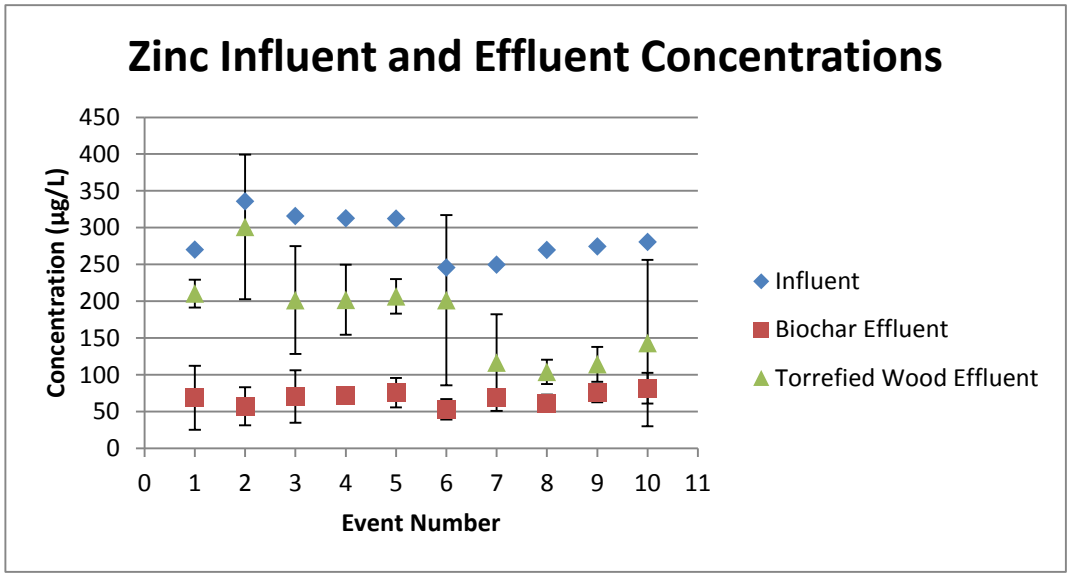

Figure 17: Average influent and effluent concentrations for 10 simulated storm events. Data is presented with 95% CI.

Effluent pH was evaluated in an effort to better understand the observed increasing percent removal for columns containing torrefied wood. The data in Figure 18 shows the relationship between effluent pH and percent metal removal. Through ten simulated storm events, the Biochar effluent pH remained within a range of 6.5 to 6.7, and percent removal held relatively constant at about 90% Cu and 75% Zn. Conversely, the Torrefied Wood effluent pH increased from 4 to 5.5 from the first to the tenth event. Increased Cu and Zn removal accompanied the increase in pH. It is known that low pH levels contribute to metal dissolution and mobility while many removal processes occur more readily at higher pH levels (Watts, 1998). Additionally, when understanding a weak acid ion exchange system it is beneficial to know whether the carboxylic acid functional groups are present in their acid or conjugate base form because conjugate bases are responsible for metal sequestration. It is likely that the increased metal removal is a result of pH increasing compared to the torrefied wood pK_a value. As this occurred, a higher percentage of carboxyl acids became available for ion exchange as their conjugate base forms. Though not performed in this study, the pK_a value of a material can be determined by acid-base titration (Su, 2012).

A possible explanation for the increase in pH is that the torrefied wood contain residual tars and organic matter, present in pyroligneous acid, that were volatilized in the higher temperature used to produce biochar (Downy et al., 2012). As each event flushes pyroligneous acid from the torrefied wood, less is present in each subsequent event, resulting in a less acidic effluent and higher pH.

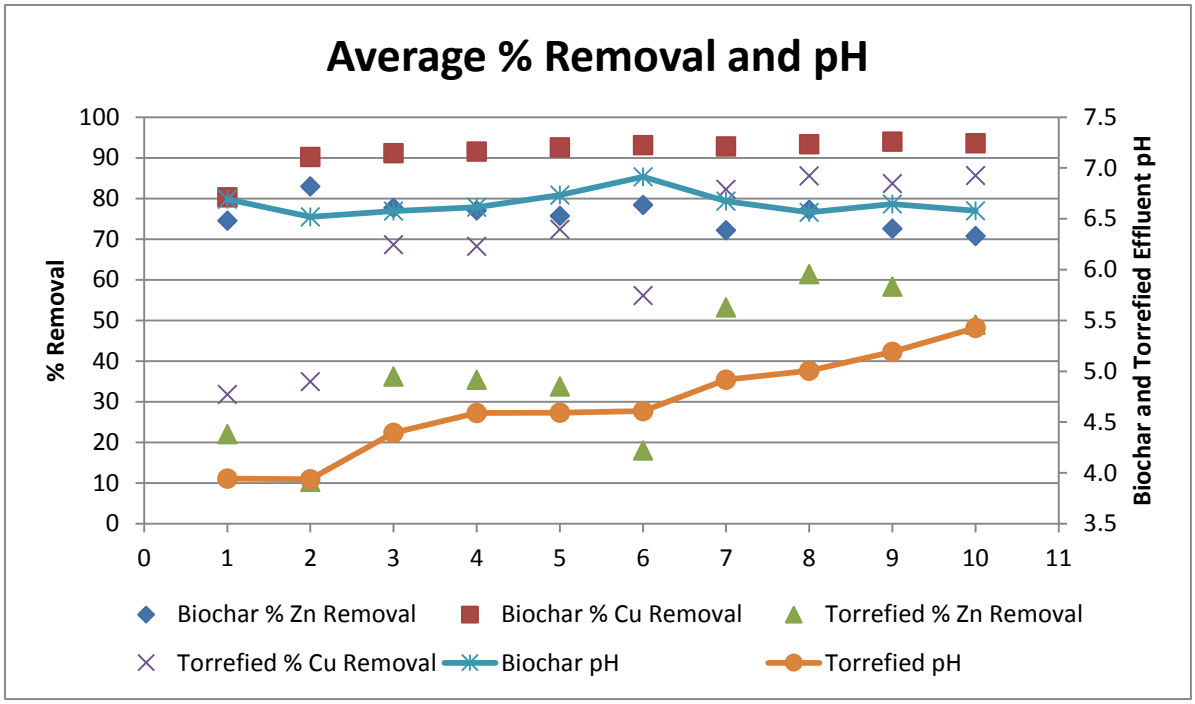

Figure 18: Average effluent pH and average percent removal of Cu and Zn as functions of storm event number.

4 CONCLUSIONS

The purpose of this study was to characterize and assess the metal (Cu and Zn) adsorption abilities of torrefied wood and biochar. CO_2 adsorption isotherms showed that the biochar surface area is about 100 times greater than that of torrefied wood due to the opening of the biochar inner pore structure and the formation of micropores. FTIR spectra revealed the formation of carboxylic acid, which can enhance sorption through ion exchange, on both torrefied wood and biochar (Figure 7). Considering the surface area and the presence of surface functional groups responsible for adsorption sites, biochar could be considered as a low cost replacement for GAC.

Single-solute Cu adsorption equilibrium tests revealed that biochar outperformed torrefied wood at low liquid phase equilibrium concentrations and had Freundlich K_F values of 0.509 and 0.412 mg/g, respectively. However, torrefied wood outperformed biochar in single-solute Zn adsorption and had Freundlich K_F values of 0.317 and 0.136 mg/g, respectively. Additionally, multi-solute (Cu and Zn) adsorption experiments showed that for both torrefied wood and biochar, Cu outcompeted Zn in a competitive sorption environment. For comparison, values of K_F for Cu and Zn sorption to GAC have been reported as 0.37 and 0.91 mg/g, respectively (Genc-Fuhrman et al., 2007). Torrefied wood and biochar have potential as metal sorbents based on single-solute isotherm performance comparisons to commonly used sorbents.

Continuous flow column studies showed that biochar had average removals of 91% Cu and 76% Zn, and torrefied wood had 67% Cu and 37% Zn average removals. While biochar yielded greater overall percent metal removals, an interesting trend was noticed regarding

column effluent pH. The percent removals and effluent pH (around 6.5) for biochar columns were relatively consistent throughout the 10 simulated events. Conversely, the percent removals for torrefied wood columns increased as event number increased. This corresponded to an increase in pH from 4 in event 1 to 5.5 in event 10. It is believed that the increasing pH resulted in increasing percent removals.

Based on the findings of this study, both torrefied wood and biochar are promising sorbents for removing Cu and Zn from stormwater runoff. Additional column testing should be performed to determine effects from effluent pH change and to find contaminant breakthrough and column exhaustion. These parameters can be used to determine sorbent lifespan. Column testing with simulated stormwater containing sediment and/or a buffered simulated stormwater could provide a closer representation of removal in a field setting. Prior to implementation, a field-scale pilot column should be used to identify potential operational issues such as media clogging, temperature effects, and to define real world metal concentration reduction.

5 WORKS CITED

ASTM Standard D2423, 1968 (2000). Standard Test Method for Permeability of Granular Soils (Constant Head). *ASTM International*, West Conshohocken, PA, 2000. www.astm.org

Barrett, M.E., Irih, L.B., Malina, J.F., Charbeneau, R.J., 1998. Characterization of Highway Runoff in Austin, Texan Area. *J. Environ. Eng.*, 124:131-137.

Chen, Q., Zhou, J., Liu, B., Mei, Q., and Lou, Z.Y., 2011. Influence of Torrefaction Pretreatment on Biomass Gasification Technology.

Chen, Y., Liu, B., Yang, H., Yang, Q., Chen, H., 2014. Evolution of Functional Groups and Pore Structure During Cotton and Corn Stalks Torrefaction and its Correlation with Hydrophobicity. *Fuel*, 137 (2014) 41-49.

Colom, X., Carrillo, F., Nogues, F., Garriga, P., 2003. Structural Analysis of Photodegraded Wood by Means of FTIR Spectroscopy. *Polym. Degrad. Stabil.*, 80 (2003) 543-549.

Crittenden, John C., Trussell, R. Rhodes, Hand, David W., Howe, Kerry J., Tchobanolous, George, 2012. Water Treatment Designs and Principles, third edition. John Wiley & Sons, Inc. Hoboken, New Jersey.

Czernik, S. and Bridgewater, A.V., 2004. Overview of Applications of Biomass Fast Pyrolysis Oil. *Energ. Fuel*., 18, 590-598.

Davis, Allen, Mohammad Shokouhian, and Shubei Ni., 2001. Loading Estimates of Lead, Copper, Cadmium, and Zinc in Urban Runoff from Specific Sources. *Chemosphere*, 44: 997-1009.

Downy, A., Cowie, A. L., and van Zwieten, L., 2012. Biochar as a Geoengineering Climate Solution: Hazard Identification and Risk Management. *Crit. Rev. Env. Sci. Tec.*, 42(3): 225-250.

Dumroese, R. K., Heiskanen, J, Englund, K, Tervahauta, A., 2011. Pelleted biochar: Chemical and Physical Properties Show Potential Use as a Substrate in Container Nursuries. *Biomass Bioenerg.*, 35 (2011) 2018-2027.

Englund, K., and Dumroese, D., Feb. 2015, Personal Communication.

EPA Method 200.7, 1994, Determination of Metals and Trace Elements in Water and Wastes by Inductively Coupled Plasma-Atomic Emission Spectrometry, Revision 4.4.

Genc-Fuhrman, Hulya, Mikkelsen, Peter S., Ledin, Anna, 2007. Simultaneous Removal of As, Cd, Cr, Cu, Ni, and Zn from stormwater: Experimental Comparison of 11 Different Sorbents. *Water Res.*, 591-602.

Giardina, Andrea, Larson, Sandra F., Wisner, Brian, Wheeler, John, Chao, Matthew, 2007. Long-term and Acute Effects of Zinc Contamination of a Stream on Fish Mortality and Physiology. *Environ. Toxicol. Chem.*, 29(2):287-295.

Haoxi, B. and Ragauskas, A.J., 2011. Torrefaction of Loblolly Pine. *Green Chem.*, 14 (2012) 72-76.

Harju, L., Lill, J.O., Saarela, K.E., Heselius, S.J., Hernberg, F.J., Lindroos, A., 1996. Study of Seasonal Variations of Trace-element Concentrations Within Tree Rings by Thick-target PIXE Analyses. *Nucl. Instrum. Meth. B,* 109-110:536-541.

Ho, Y.S., Huang, C.T., Huang, H.W., 2002. Equilibrium Sorption Isotherm for Metal Ions on Tree Fern. *Process Biochem.*, 1421-1430.

Jones, J.M., Bridgeman, T.G., Darvell, L.I., Gudka, B., Saddawi, A., Williams, A., 2012. Combustion Properties of Torrefied Willow Compared with Bituminous Coals. *Fuel Proc. Tec.*, 101: 1-9.

Karami, N., Clemente, R., Moreno-Jimenez, E., Lepp, N.W., Beesley, L., 2011. Efficiency of Green Waste Compost and Biochar Soil Amendments for Reducing Lead and Copper Mobility and Uptake to Ryegrass. *J. Hazard. Mater.*,191 (2011) 41-48.

Kayhanian, M., Suverkropp, C., Ruby, A., and Tsay, K., 2006. Characterization and Prediction of Highway Runoff Constituent Event Mean Concentration. *J. Environ. Manage.*, 85(2):279-295.

Kestin, J., Sokolov, M., and Wakeham, W.A., 1978. Viscosity of Liquid Water in the Range -8°C to 150°C. *J. Phys. Chem.*, Ref. Data, 7(3):941-948.

Kori-Siakpere, Ovie, and Ewoma Oghoghene Ubogu, 2008. Sublethal Haematological Effects of Zinc on the Freshwater Fish, Heteroclaria sp. *Afr J.Biotechnol.*,7.12: 2068-2073.

Lehmann, Johannes, 2007. Bio-energy in the Black. *Front. Ecol. Environ.* 5(7):381-387.

Liu, D., Sansalone, J.J., Cartledge, F.K., 2005. Comparison of Sorptive Filter Media for Treatment of Metals in Runoff. *J. Environ. Eng.*, 131:1178-1186.

Marsalek, J., Brownlee, B., Mayer, T., Lawal, S., Larkin, G., 1997. Heavy Metals and PAHs in Stormwater Runoff from the Skyway Bridge, Burlington, Ontario. *Water Qual. Res. J. Can.,* 32(4):815-827.

Mohan, Dinesh, Singh, Kunwar P., 2004. Single- and Multi-component Adsorption of Cadmium and Zinc Using Activated Carbon Derived from Bagasse – an Agricultural Waste. *Water Res.,* 2304-2318.

Park, J., Meng, J., Lim, K.H., Rojas, O.J. Park, S., 2013. Transformation of Lignocellulosic Biomass During Torrefaction. *J. Anal. Appl. Pyrol.,* 100 (2013) 199-206.

Phanphanich, M. and Mani, S., 2011. Impact of Torrefaction on the Grindability and Fuel Characteristics of Forest Biomass. *Bioresource Technol.,* 102 (2011) 1246-1253.

Prins, M.J., Ptasinski, K.J., Frans J.J., Janssen, G., 2006. More Efficient Biomass Gasification via Torrefaction. *Energy,*31 (2006) 3458-3470.

Sandahl, Jason F., David H. Baldwin, Jeffrey J. Jenkins, and Nathaniel L. Scholz, 2007. A Sensory System At The Interface Between Urban Stormwater Runoff And Salmon Survival. *Environ. Sci. Technol.,* 41.8: 2998-3004. Print.

Sansalone, John J., and Steven G. Buchberger, 1997. Partitioning And First Flush Of Metals In Urban Roadway Storm Water. *J. Environ. Eng.,* 123.2 (1997): 134.

Su, Pingping, 2012, Sorption of Metal Ions to Wood, Pulp, and Bark Materials. Abo Akademi University, 81 pages.

Toles, C.A., Marshall, W.E., and Johns, M.M., 1999. Surface Functional Groups on Acid-activated Nutshell Carbons. *Carbon,* 37:1207-1214.

Tong, X., Li, J., Yuan, J., Xu, R., 2011. Adsorption of Cu(II) by Biochars Generated From Three Crop Straws. *Chem. Eng. J.,* 172 (2011) 828-834.

USEPA. Preliminary Data Summary of Urban Stormwater Best Management Practices. EPA–821–R–99–012 (1999) Chapter 4.

Washington Administrative Code 173-201A-240. 2013. Update 5/9/11. Retrived from http://apps.leg.wa.gov/WAC/default.aspx?cite=173-201A-240.

Watts, R.J., 1998. Hazardous Wastes: Sources, Pathways, Receptors. John Wiley & Sons, Inc. New York, New York.

Wisdom, Charlie, and Paul Bucich, 15 Apr. 2011. Dissolved Metals in Stormwater. *The Water Report.* 1-15.

WSDOT, IST Charrette Literature Review, SR 520 Corridor Program. *Washington State Department of Transportation*, 2009.

Wu, Jy S., Craig J. Allan, William L. Saunders, and Jack B. Evett, 1998. Characterization And Pollutant Loading Estimation For Highway Runoff. *J. Environ. Eng.* 124.7: 584.

Yonge, David, and Roelen, Piper, 2003. An Evaluation of Stormwater Permeable Rapid Inflitration Barriers for Use in Class V Stormwater Injection Wells. *WSDOT Research Project T1804-10*.

Yonge, D., Hossain, A., Barber, M., and Chen, S., Griffin, D., 2002. Wet Detention Pond Design for Highway Runoff Pollutant Control. *National Cooperative Highway Research Program Transportation Research Board*, 25-12.

Yu, B., Zhang, Y., Shukla, A., Shukla, S.S., Dorris, K.L., 2000. The Removal of Heavy Metal from Aqueous Solutions by Sawdust Adsorption—Removal of Copper. *J. Hazard. Mater.* 80(1-3):33-42.

6 APPENDIX

6.1 APPENDIX A – ISOTHERM PH ADJUSTMENT

The pH of adsorption equilibrium and kinetics experiments was adjusted with predetermined volumes of 1 M HNO_3 or 1 M NaOH. After a known mass of material and a specified volume of acid or base was added to a bottle, the sample was mixed on a rotating table for a known time for pH equilibration. After pH equilibration, metals were added to samples for adsorption tests (see chapter 2.4 for specific procedures). Tables and graphs presented in this appendix show volumes of acid or base added to bottles, and the pH response as a function of contact time with materials.

Table 6: pH as a function of contact time with the biochar.

Time, min	**pH**	**Time, hrs**
18	3.3	0.30
36	3.75	0.60
56	4.08	0.93
76	4.35	1.27
99	4.58	1.65
131	4.87	2.18
286	5.47	4.77
1225	6.23	20.42
1404	6.34	23.40
1519	6.41	25.32
1699	6.43	28.32
1861	6.53	31.02
2786	6.63	46.43

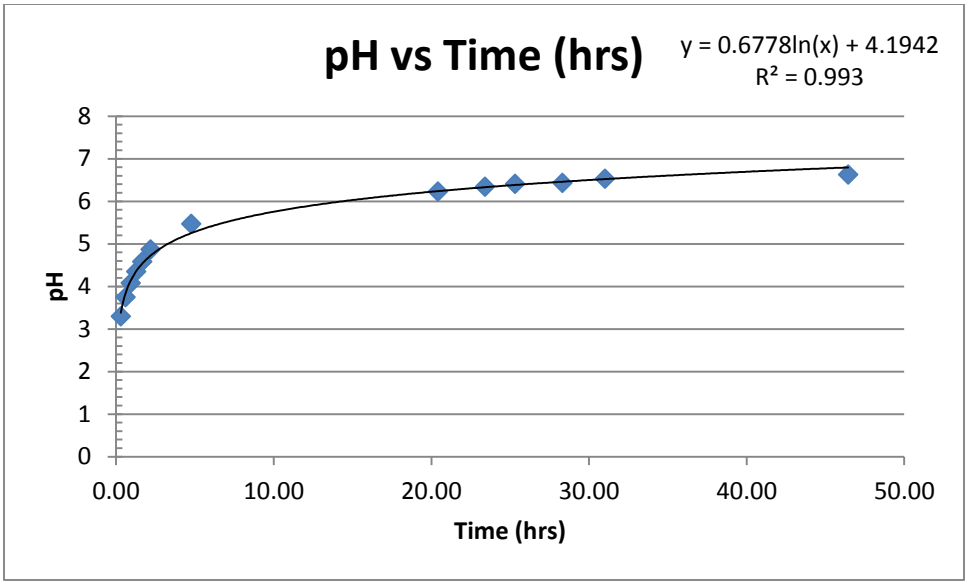

Figure 19: pH as a function of contact time with a 5g sample of biochar. It was decided that a 14 hour pH equilibration period would be used for all biochar samples.

Table 7: HNO_3 volumes added to single-solute biochar isotherm bottles.

	Biochar Cu	**Biochar Zn**
mass (g)	**volume HNO3 (uL)**	**volume HNO3 (uL)**
1	75	100
2	200	250
3	350	400
4	500	550
5	650	700

Table 8: HNO_3 volumes added to multi-solute biochar isotherm bottles.

	Biochar
mass (g)	**volume HNO3 (uL)**
1	100
2	250
3	400
4	550
5	700

200 mL HNO_3 were added to all biochar kinetic tests

Table 9: pH as a function of contact time with torrefied wood.

tim, min	pH	time, hrs
0	3.39	0.00
17	9.98	0.28
37	9.2	0.62
59	8.5	0.98
92	7.95	1.53
131	7.51	2.18
197	7.18	3.28
243	7	4.05
357	6.81	5.95
496	6.63	8.27
664	6.5	11.07
1396	6.26	23.27
1508	6.19	25.13
1600	6.26	26.67
1747	6.17	29.12
2923	6	48.72

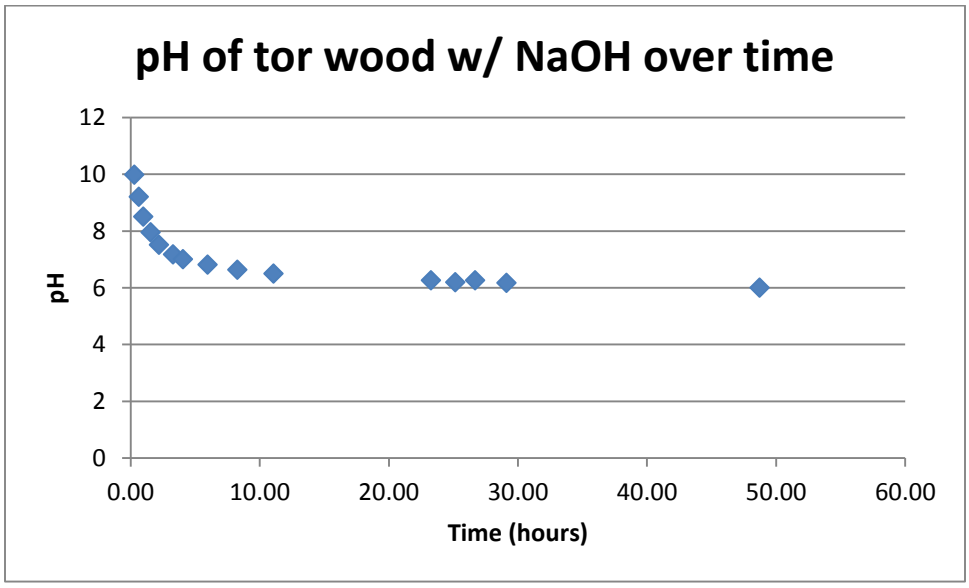

Figure 20: pH as a function of contact time with a 5g sample of torrefied wood. It was decided that an 8 hour pH equilibration time would be used for torrefied wood samples.

Table 10: NaOH volumes added to single-solute torrefied wood isotherm bottles.

	Torrefied wood Cu	**Torrefied Wood Zn**
mass (g)	**volume NaOH (uL)**	**volume NaOH (uL)**
1	200	175
2	375	350
3	550	525
4	725	700
5	900	875

Table 11: NaOH volumes added to multi-solute torrefied wood isotherm bottles.

	Biochar
mass (g)	**volume HNO3 (uL)**
1	175
2	350
3	525
4	700
5	875

270 mL NaOH were added to all torrefied wood kinetics tests.

6.2 APPENDIX B – DATA

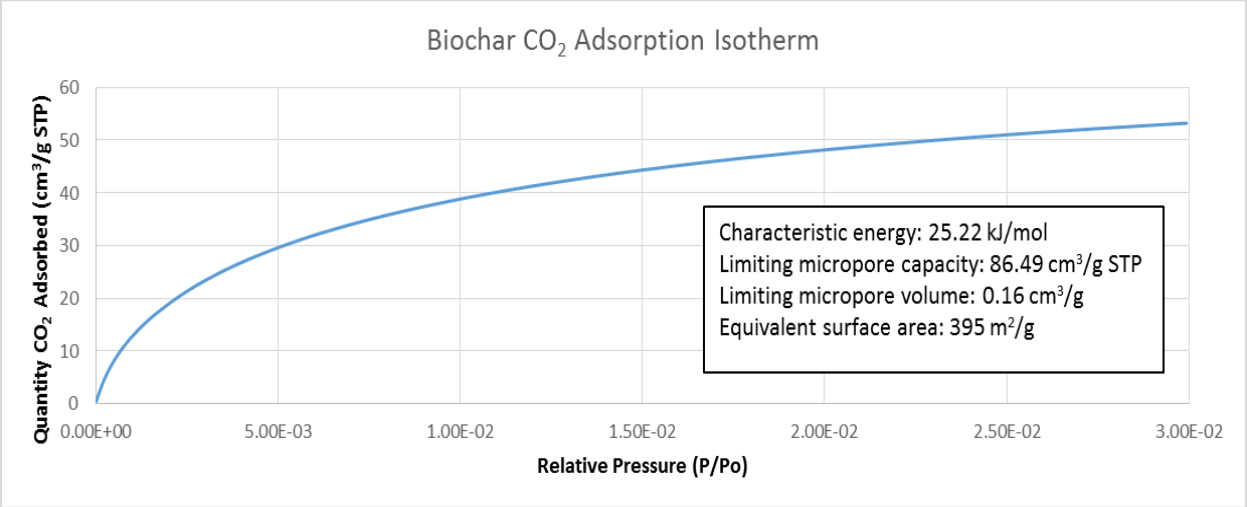

Figure 21: Biochar CO_2 adsorption isotherm detailing the Quantity of Adsorbed CO_2 as a function of Relative Pressure. The equivalent surface area was calculated to be 395 m^2/g.

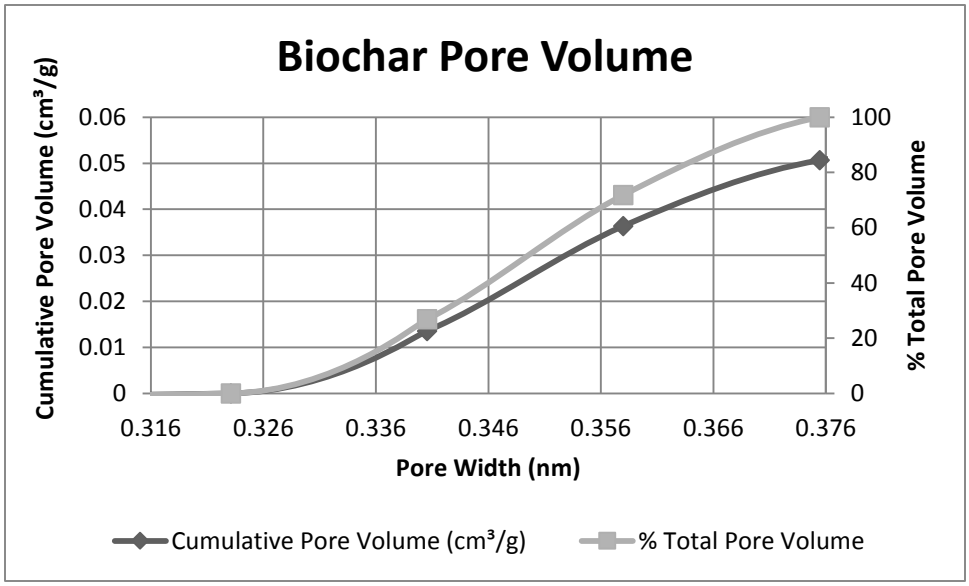

Figure 22: Biochar micropore volume distribution.

Table 12: Complete results from microwave digestion analysis.

	Concentration (µg/g)		
Analyte	**Raw Wood**	**Torrefied Wood**	**Biochar**
Al	BDL	24	750
As	BDL	BDL	BDL
Ba	8	10	92
Ca	44	270	7770
Co	BDL	BDL	BDL
Cr	BDL	BDL	3

Cu	BDL	26	10
Fe	20	30	730
K	130	40	2670
Mg	160	20	2130
Mn	10	9	400
Na	BDL	BDL	270
Ni	BDL	BDL	2
Pb	BDL	5	BDL
V	BDL	BDL	2
Zn	5	2	38

Table 13: Biochar single-solute isotherm equilibrium data.

Biochar, single-solute Cu						
mass sorbent, g	**Co, mg/L**	**Ce, mg/L**	**qe, mg/g**	**Average qe**	**Average Ce**	**Eq. pH**
1	6.87	2.61	0.85	0.77	3.00	6.26
1	6.87	3.40	0.69			6.18
2	6.87	1.35	0.55	0.55	1.35	6.37
3	6.87	0.50	0.42	0.43	0.49	6.37
3	6.87	0.48	0.43			6.42
4	6.87	0.33	0.33	0.33	0.33	6.43
5	6.87	0.21	0.27	0.27	0.20	6.42
5	6.87	0.25	0.26			6.39
5	6.87	0.15	0.27			6.53
Biochar, single-solute Zn						
mass sorbent, g	**Co, mg/L**	**Ce, mg/L**	**qe, mg/g**	**Average qe**	**Average Ce**	**Eq. pH**

1	10.00	7.04	0.59	0.63	6.83	6.24
1	10.00	6.43	0.71			6.41
1	10.00	7.02	0.60			6.28
2	10.00	5.29	0.47	0.47	5.29	6.32
3	10.00	3.84	0.41	0.40	3.93	6.50
3	10.00	4.14	0.39			6.43
3	10.00	3.82	0.41			6.50
4	10.00	2.69	0.37	0.37	2.69	6.62
5	10.00	2.69	0.29	0.29	2.71	6.57
5	10.00	2.79	0.29			6.53
5	10.00	2.64	0.29			6.58
7	7.73	1.78	0.17	0.17	1.78	6.75

Table 14: Torrefied wood single-solute isotherm equilibrium data.

Torrefied Wood, single-solute Cu						
mass sorbent, g	**Co, mg/L**	**Ce, mg/L**	**qe, mg/g**	**Average qe**	**Average Ce**	**Eq pH**
1	7.00	2.87	0.83	0.79	3.07	5.91
1	7.00	3.09	0.78			5.82
1	7.00	3.24	0.75			5.85
2	7.00	1.62	0.54	0.54	1.62	5.85
3	7.00	0.97	0.40	0.41	0.89	5.99
3	7.00	0.85	0.41			6.08
3	7.00	0.84	0.41			6.18
4	7.00	0.59	0.32	0.32	0.59	6.24
5	7.00	0.59	0.26	0.26	0.56	6.05
5	7.00	0.53	0.26			6.12
5	7.00	0.55	0.26			6.15
Torrefied Wood, single-solute Zn						
mass sorbent, g	**Co, mg/L**	**Ce, mg/L**	**qe, mg/g**	**Average qe**	**Average Ce**	**Eq. ph**
1	10.01	6.87	0.63	0.71	6.48	6.11
1	10.01	6.38	0.73			6.18
1	10.01	6.20	0.76			6.24
2	10.01	3.64	0.64	0.64	3.64	6.22
3	10.01	1.89	0.54	0.55	1.80	6.36
3	10.01	1.65	0.56			6.38

3	10.01	1.87	0.54			6.38
4	10.01	1.58	0.42	0.42	1.58	6.47
5	10.01	1.80	0.33	0.34	1.57	6.18
5	10.01	1.11	0.36			6.39
5	10.01	1.81	0.33			6.20
7	10.01	0.90	0.26	0.26	0.90	6.45
9	10.01	0.81	0.20	0.20	0.81	6.32

Table 15: Biochar multi-solute equilibrium isotherm data.

Biochar (competitve) Cu						
mass sorbent, g	**Co, mg/L**	**Ce, mg/L**	**qe, mg/g**	**Average qe**	**Average Ce**	**Eq. pH**
1	2.45	0.30	0.43	0.44	0.26	6.35
1	2.45	0.29	0.43			6.33
1	2.45	0.20	0.45			6.51
2	2.45	0.10	0.23	0.23	0.10	6.44
3	2.45	0.05	0.16	0.16	0.06	6.54
3	2.45	0.07	0.16			6.37

3	2.45	0.05	0.16			6.51
4	2.45	0.03	0.12	0.12	0.03	6.70
5	2.45	0.03	0.10	0.10	0.02	6.47
5	2.45	0.02	0.10			6.59
5	2.45	0.02	0.10			6.63
Biochar (competitve) Zn						
mass sorbent, g	**Co, mg/L**	**Ce, mg/L**	**qe, mg/g**	**Average qe**	**Average Ce**	**Eq. pH**
1	4.76	3.55	0.24	0.26	3.47	6.35
1	4.76	3.70	0.21			6.33
1	4.76	3.15	0.32			6.51
2	4.76	2.61	0.22	0.22	2.61	6.44
3	4.76	1.73	0.20	0.18	1.99	6.54
3	4.76	2.31	0.16			6.37
3	4.76	1.92	0.19			6.51
4	4.76	1.11	0.18	0.18	1.11	6.70
5	4.76	1.48	0.13	0.14	1.26	6.47
5	4.76	1.14	0.14			6.59
5	4.76	1.15	0.14			6.63

Table 16: Torrefied wood multi-solute equilibrium isotherm data.

Torrefied Wood (competitve) Cu						
mass sorbent, g	Co, mg/L	Ce, mg/L	qe, mg/g	Average qe	Average Ce	Eq. pH
1	2.45	0.66	0.36	0.36	0.67	6.22
1	2.45	0.71	0.35			6.16
1	2.45	0.64	0.36			6.18
2	2.45	0.34	0.21	0.21	0.34	6.28
3	2.45	0.28	0.14	0.14	0.27	6.13
3	2.45	0.27	0.14			6.21
3	2.45	0.27	0.15			6.27
4	2.23	0.14	0.10	0.10	0.14	5.72
5	2.45	0.17	0.09	0.09	0.17	6.33
5	2.45	0.17	0.09			6.37
5	2.45	0.17	0.09			6.27
Torrefied Wood (competitve) Zn						

mass sorbent, g	Co, mg/L	Ce, mg/L	qe, mg/g	Average qe	Average Ce	Eq. pH
1	4.76	3.24	0.30	0.31	3.23	6.22
1	4.76	3.28	0.30			6.16
1	4.76	3.16	0.32			6.18
2	4.76	1.75	0.30	0.30	1.75	6.28
3	4.76	1.60	0.21	0.22	1.40	6.13
3	4.76	1.37	0.23			6.21
3	4.76	1.24	0.23			6.27
4	3.69	0.41	0.16	0.16	0.41	5.72
5	4.76	0.68	0.16	0.16	0.68	6.33
5	4.76	0.65	0.16			6.37
5	4.76	0.72	0.16			6.27

Table 17: Biochar kinetics data.

Biochar Cu						
Sample #	Time, hrs	Co, ppm	Eq. pH	Ct, ppm	% removal	average % removal
44	6	2.55	6.02	0.76	70.09	69.64
45	6	2.55	5.91	0.80	68.58	
46	6	2.55	5.90	0.76	70.24	
47	12	2.55	6.02	0.39	84.85	83.00
48	12	2.55	6.11	0.52	79.44	
49	12	2.55	6.15	0.39	84.71	
50	24	2.55	6.06	0.27	89.36	89.29
51	24	2.55	6.18	0.24	90.49	
52	24	2.55	6.09	0.31	88.00	
53	48	2.55	6.36	0.11	95.85	95.03
54	48	2.55	6.29	0.13	94.97	
55	48	2.55	6.32	0.15	94.27	
56	72	2.55	6.30	0.08	96.71	96.37
57	72	2.55	6.29	0.09	96.28	
58	72	2.55	6.33	0.10	96.11	

Biochar Zn						
Sample #	Time, hrs	Co, ppm	Eq. pH	Ct, ppm	% removal	average % removal
44	6	4.70	6.02	3.95	16.07	13.89
45	6	4.70	5.91	4.09	13.03	
46	6	4.70	5.90	4.11	12.57	
47	12	4.70	6.02	3.80	19.18	20.36
48	12	4.70	6.11	3.91	16.79	
49	12	4.70	6.15	3.52	25.10	
50	24	4.70	6.06	3.61	23.17	24.91
51	24	4.70	6.18	3.37	28.25	
52	24	4.70	6.09	3.60	23.32	
53	48	4.70	6.36	2.71	42.27	36.11
54	48	4.70	6.29	3.07	34.79	
55	48	4.70	6.32	3.23	31.27	
56	72	4.70	6.30	2.88	38.64	38.78
57	72	4.70	6.29	2.84	39.61	
58	72	4.70	6.33	2.91	38.09	

Table 18: Torrefied wood kinetics data.

Torrefied Wood Cu						
Sample #	Time, hrs	Co, ppm	Eq. pH	Ct, ppm	% removal	average % removal
26	6	2.47	6.19	0.81	67.36	70.43
27	6	2.47	6.40	0.69	72.22	
28	6	2.47	6.40	0.70	71.71	
32	12	2.47	6.28	0.45	81.78	81.91
33	12	2.47	6.38	0.42	82.98	
34	12	2.47	6.35	0.47	80.97	
35	24	2.47	6.01	0.43	82.54	81.41
36	24	2.47	5.79	0.66	73.19	
37	24	2.47	6.29	0.28	88.50	
38	48	2.47	5.90	0.27	89.03	87.98
39	48	2.47	5.80	0.30	87.73	
40	48	2.47	5.89	0.32	87.17	

41	72	2.47	6.08	0.20	91.85	92.09
42	72	2.47	6.03	0.21	91.56	
43	72	2.47	6.16	0.18	92.87	
Torrefied Wood Zn						
Sample #	Time, hrs	Co, ppm	Eq. pH	Ct, ppm	% removal	average % removal
26	6	4.55	6.19	2.92	35.75	42.61
27	6	4.55	6.40	2.37	47.92	
28	6	4.55	6.40	2.54	44.15	
32	12	4.55	6.28	2.08	54.34	57.48
33	12	4.55	6.38	1.72	62.20	
34	12	4.55	6.35	2.01	55.91	
35	24	4.55	6.01	2.52	44.60	47.58
36	24	4.55	5.79	3.12	31.38	
37	24	4.55	6.29	1.51	66.77	
38	48	4.55	5.90	2.20	51.59	47.27
39	48	4.55	5.80	2.58	43.23	
40	48	4.55	5.89	2.41	46.98	
41	72	4.55	6.08	1.55	65.83	66.21
42	72	4.55	6.03	1.69	62.95	
43	72	4.55	6.16	1.37	69.85	

Table 19: Hydraulic conductivity data for raw wood, torrefied wood, and biochar.

Raw Wood								
	Temp (°C)	Length (in.)	Dia. (in)	Area (in^2)	k ave tot (cm/s)	k Temp adjust (cm/s)		
	16.5	7.9375	3.94	12.18	0.336	0.368		
Trial	Run	Vol. (mL)	Vol. (in^3)	Δh (in.)	Δt (sec.)	k (in/s)	k (cm/s)	k temp adj (cm/s)
1	A	1120	68.35	64.375	5.11	0.135	0.344	0.377
	B	1145	69.87		5.16	0.137	0.348	0.381
	C	1215	74.14		5.73	0.131	0.333	0.364
2	A	1300	79.33	61.3125	6.22	0.136	0.344	0.377
	B	1520	92.76		7.26	0.136	0.345	0.378
	C	1400	85.43		6.78	0.134	0.340	0.373
3	A	1565	95.50	58.3125	8.11	0.132	0.334	0.366
	B	1360	82.99		7.06	0.131	0.334	0.366
	C	1825	111.37		9.67	0.129	0.327	0.358
4	A	1530	93.37	55.25	8.17	0.135	0.342	0.375
	B	1530	93.37		8.16	0.135	0.343	0.376
	C	1555	94.89		8.81	0.127	0.323	0.354
5	A	1770	108.01	52.25	9.86	0.137	0.347	0.380
	B	1260	76.89		7.34	0.128	0.324	0.355
	C	1530	93.37		9.1	0.125	0.317	0.348
Torrefied Wood								
	Temp (°C)	Length (in.)	Dia. (in)	Area (in^2)	k ave tot (cm/s)	k Temp adjust (cm/s)		
	14	7.90625	3.94	12.18	0.307	0.359		
Trial		Vol. (mL)	Vol. (in^3)	Δh (in.)	Δt (sec.)	k (in/s)	k (cm/s)	k temp adj
1	A	895	54.62	64	4.38	0.127	0.321	0.376
	B	910	55.53		4.54	0.124	0.315	0.369
	C	1000	61.02		5	0.124	0.315	0.368
2	A	1160	70.79	61	6.05	0.125	0.316	0.370
	B	1000	61.02		5.17	0.126	0.319	0.373

	C	1350	82.38		7.1	0.124	0.314	0.367
3	A	1460	89.09	58	8.25	0.121	0.307	0.359
	B	1800	109.84		10.3	0.119	0.303	0.355
	C	1440	87.87		8.11	0.121	0.308	0.360
4	A	1480	90.31	55	8.77	0.122	0.309	0.361
	B	1630	99.47		10	0.117	0.298	0.349
	C	1700	103.74		10.41	0.118	0.299	0.350
5	A	1330	81.16	52	8.64	0.117	0.298	0.348
	B	1680	102.52		10.94	0.117	0.297	0.348
	C	1440	87.87		9.72	0.113	0.287	0.335

Biochar

	Temp (°C)	Length (in.)	Dia. (in)	Area (in^2)	k ave tot (cm/s)	k Temp adjust (cm/s)		
	12.5	8	3.94	12.18	0.548	0.669		
Trial		Vol. (mL)	Vol. (in^3)	Δh (in.)	Δt (sec.)	k (in/s)	k (cm/s)	k temp adj
1	A	1060	64.69	64.0625	3.09	0.215	0.545	0.665
	B	1100	67.13		3.36	0.205	0.520	0.635
	C	1075	65.60		3.35	0.201	0.510	0.622
2	A	1130	68.96	61.0625	3.42	0.217	0.551	0.672
	B	950	57.97		2.91	0.214	0.544	0.664
	C	1400	85.43		4.32	0.213	0.540	0.659
3	A	1160	70.79	58.0625	3.67	0.218	0.554	0.676
	B	1215	74.14		3.82	0.220	0.558	0.681
	C	1020	62.24		3.33	0.212	0.537	0.656
4	A	1030	62.85	55.0625	3.42	0.219	0.557	0.680
	B	1140	69.57		3.96	0.210	0.532	0.650
	C	1310	79.94		4.31	0.221	0.562	0.686
5	A	1060	64.69	52.0625	3.64	0.224	0.570	0.695
	B	1190	72.62		4.12	0.222	0.565	0.689
	C	1180	72.01		4.01	0.227	0.576	0.702

Table 20: Adsorption column testing data for biochar (B1, B2, and B3) and torrefied wood (T1, T2, T3).

Concentration (µg/L)														
	Influent		B1		B2		B3		T1		T2		T3	
Event	zn	cu	zn	cu	zn	cu	zn	cu	zn	cu	zn	cu	zn	cu
1	270.0	45.0	90.2	13.5	68.6	6.1	47.5	7.0	209.3	23.7	220.3	34.3	201.7	34.0
2	336.0	63.0	63.2	9.4	66.0	5.3	42.6	3.8	247.4	31.8	314.9	42.2	341.4	48.8
3	316.0	57.0	81.9	4.8	79.1	6.4	50.2	4.0	162.2	13.9	233.2	23.2	209.3	16.5
4	312.9	58.4	69.7	4.8	76.6	5.3	69.0	4.8	223.2	18.8	206.0	20.4	176.9	16.4
5	312.4	66.8	72.7	5.2	86.9	5.5	67.8	4.2	193.6	14.6	212.1	20.2	214.8	20.4
6	246.0	52.1	60.8	3.9	50.8	3.4	47.6	3.5	157.6	15.2	266.1	32.9	181.0	20.4
7	249.5	57.6	67.4	3.7	73.0	4.5	67.9	4.2	79.3	5.5	133.6	13.1	137.0	12.1
8	269.7	48.8	57.8	2.5	58.4	2.9	68.0	4.3	94.8	6.2	106.8	7.1	110.5	7.8
9	274.3	53.7	68.2	3.0	79.3	2.6	78.2	4.1	118.5	8.8	123.3	9.9	101.1	7.6
10	280.7	64.5	78.8	4.0	73.6	3.3	93.4	5.1	117.1	10.4	207.3	8.7	105.3	8.6

Table 21: Influent and effluent pH values for 10 simulated events.

pH							
Event	Influent	B1	B2	B3	T1	T2	T3
1	6.14	6.34	6.74	7	4.09	3.91	3.83
2	5.77	6.43	6.4	6.73	4.11	3.9	3.8
3	5.76	6.53	6.46	6.74	4.46	4.36	4.36
4	5.79	6.53	6.61	6.7	4.56	4.49	4.72
5	6.2	6.72	6.76	6.72	4.73	4.53	4.52
6	6.35	6.9	7.05	6.79	4.97	4.37	4.49
7	6.15	6.71	6.62	6.69	5.26	4.77	4.72
8	6.28	6.68	6.46	6.55	5.27	4.8	4.95
9	6.24	6.61	6.62	6.71	5.26	5.14	5.17
10	6.35	6.74	6.51	6.49	5.54	5.34	5.4

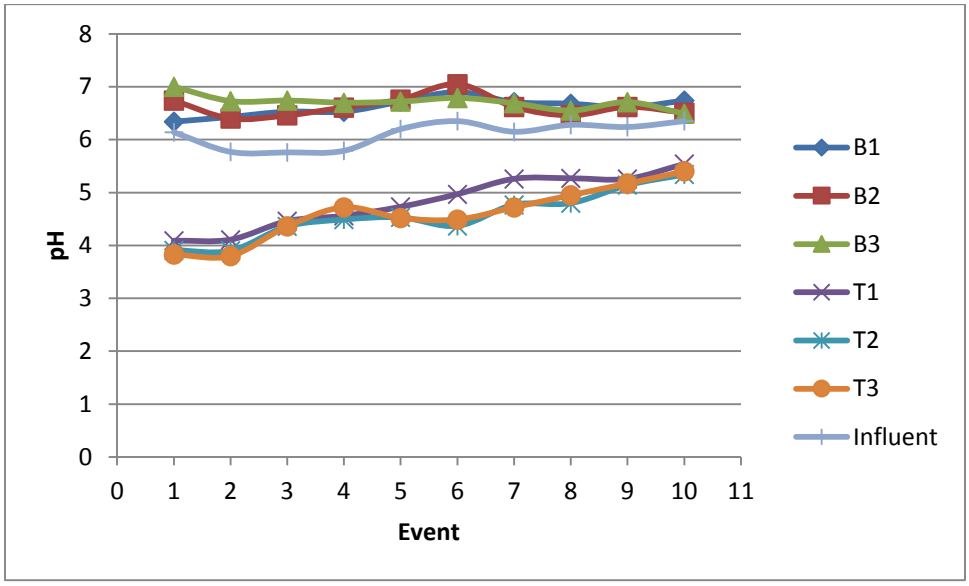

Figure 22: Influent and effluent pH for 10 simulated events.